Journal of Power Sources 521 (2022) 230859

Contents lists available at ScienceDirect

Journal of Power Sources

journal homepage: www.elsevier.com/locate/jpowsour

Review article

# Parametrization of physics-based battery models from input–output data: A review of methodology and current research

Malin Andersson [a,c,*,1], Moritz Streb [b,1], Jing Ying Ko [b], Verena Löfqvist Klass [c], Matilda Klett [b,c], Henrik Ekström [b,d], Mikael Johansson [a], Göran Lindbergh [b,**]

[a] Division of Decision and Control Systems, Department of Intelligent Systems, School of Electrical Engineering and Computer Science, KTH Royal Institute of Technology, Malvinas väg 10, 114 28 Stockholm, Sweden

[b] Applied Electrochemistry, Department of Chemical Engineering, School of Engineering Sciences in Chemistry, Biotechnology and Health, KTH Royal Institute of Technology, Teknikringen 42, 114 28 Stockholm, Sweden

[c] Scania CV AB, Granparksvägen 10, 151 48 Södertälje, Sweden

[d] COMSOL AB, Tegnérgatan 23, 111 40 Stockholm, Sweden

## GRAPHICAL ABSTRACT

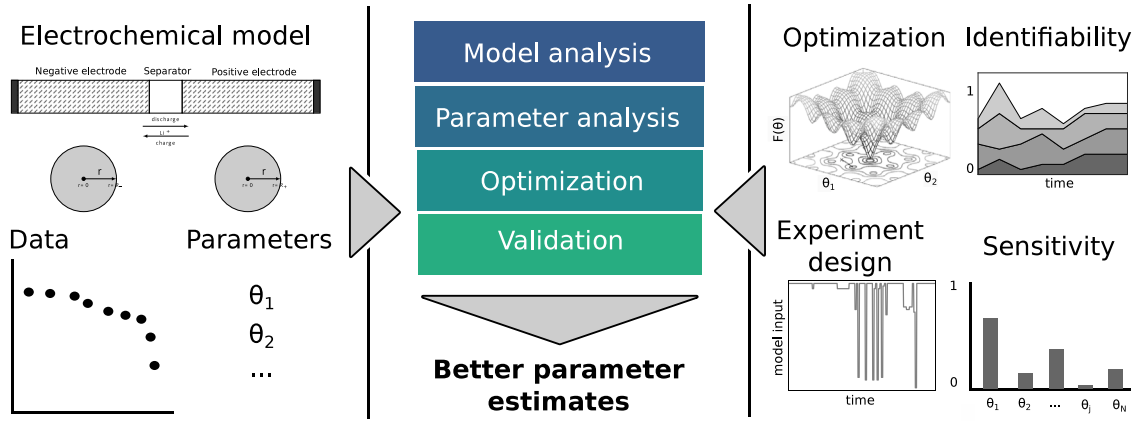


## HIGHLIGHTS

- Reviewing physics-based battery model parameter estimation.
- Discussion of sensitivity analysis, optimal experiment design and machine learning.
- Highlighting strengths and weaknesses of common techniques for parameter estimation.
- Linking electrochemical modeling and control theory.
- Elucidating importance of thorough parameter estimation procedure.

## ARTICLE INFO

*Keywords:*
Battery model

## ABSTRACT

Physics-based battery models are important tools in battery research, development, and control. To obtain useful information from the models, accurate parametrization is essential. A complex model structure and

* Corresponding author at: Division of Decision and Control Systems, Department of Intelligent Systems, School of Electrical Engineering and Computer Science, KTH Royal Institute of Technology, Malvinas väg 10, 114 28 Stockholm, Sweden.
** Corresponding author.
*E-mail addresses:* malinan9@kth.se (M. Andersson), gnli@kth.se (G. Lindbergh).
[1] These authors contributed equally.

https://doi.org/10.1016/j.jpowsour.2021.230859
Received 27 September 2021; Received in revised form 23 November 2021; Accepted 29 November 2021
Available online 13 January 2022

Parameter estimation
Optimization
Sensitivity
Identifiability
Experiment design

many unknown and hard-to-measure parameters make parametrization challenging. Furthermore, numerous applications require non-invasive parametrization relying on parameter estimation from measurements of current and voltage. Parametrization of physics-based battery models from input–output data is a growing research area with many recent publications. This paper aims to bridge the gap between researchers from different fields that work with battery model parametrization, since successful parametrization requires both knowledge of the underlying physical system as well as understanding of theory and concepts behind parameter estimation. The review encompasses sensitivity analyses, methods for parameter optimization, structural and practical identifiability analyses, design of experiments and methods for validation as well as the use of machine learning in parametrization. We highlight that not all model parameters can accurately be identified nor are all relevant for model performance. Nonetheless, no consensus on parameter importance could be shown. Local methods are commonly chosen because of their computational advantages. However, we find that the implications of local methods for analysis of non-linear models are often not sufficiently considered in reviewed literature.

## 1. Introduction

The broad variety of Li-ion battery applications has since their introduction sparked development of numerous battery models, from physics-based electrochemical descriptions to entirely data-driven representations. Battery models are used in industry and academia to evaluate cell design [1], improve quality control in battery manufacturing [2], estimate state-of-health (SOH) [3] and state-of-charge (SOC) [4], predict degradation behavior [5,6] as well as to design and evaluate control strategies [7]. The choice of model largely depends on the required resolution and the available computational resources.

Models based on physics link a system's physical properties to its behavior. In the battery development process, physics-based models are implemented e.g. to test battery design choices, before prototypes are available, and to simulate degradation rate, before lengthy aging tests are completed. During operation, Li-ion batteries must be monitored and controlled for the purpose of both safety and performance. State-of-the-art battery management systems (BMS) commonly employ empirical equivalent circuit models [8,9] for SOC and SOH estimation. The circuits are obtained by generously lumping many physical processes, e.g. resistances from many contributors into a single equivalent circuit resistance. Their low computational cost comes with the drawback that such a model cannot capture internal battery states [10]. Battery control based on internal states and electrochemically motivated limits has been proposed for applications such as electric vehicles (EVs) and grid-connected energy storage systems [11–15]. Physics-based control has been shown to increase the power and capacity utilization of the battery [15–17], but requires reliable physics-based models.

The most widely used physics-based model in literature is the Doyle-Fuller-Newman (DFN) model [18,19] that combines porous electrode theory with concentrated solution theory and describes the battery dynamics with a set of coupled partial differential algebraic equations (PDAEs). It predicts the cell voltage response to an applied current input and provides spatial resolution of internal potentials as well as lithium cation and intercalated lithium concentrations. For easier implementation in control applications, several types of reductions of this model exist. Most notable is the single particle model (SPM) [20,21].

As both the DFN model and its common reductions contain a large number of parameters, accurate parametrization is a key challenge. Even though the models are based on descriptions of the internal physical processes, not all parameters have a clear physical meaning nor can they all be measured experimentally. Traditionally, full parametrization of a cell is performed by combining physical, chemical and electrochemical characterization techniques and curve fitting [22–26]. It is a time-consuming procedure that requires the cell to be taken apart. Not all applications allow a lengthy or invasive parametrization strategy and modelers often resort to using literature values of some parameters. As the development of new battery chemistries is accelerating [27], literature values for parameters are becoming obsolete at a faster pace and can potentially yield large model errors if used. There can even be significant differences between individual cells using the same chemistry, necessitating parametrization on the specific cell of interest. This can be caused by differences in cell design, cell manufacturing [28], or material quality [29]. Additionally, the parameters of a battery will change throughout its lifetime [30], making it crucial in many applications to update the model parametrization as the battery ages. If model parameters could be identified accurately only from curve-fitting of cell voltage data, the parametrization process would be efficient, non-intrusive and suitable for most applications.

Driven by this, parametrization of physics-based battery models from observed input–output data has been the topic of many publications in recent years. This literature is the scope of the present review. While the reviewed literature is mainly limited to the DFN and SPM models, the techniques used therein and laid out in this review are valid for any parameter estimation study. Many of the used methods, along with the underlying theory, originate from the fields of control, optimization and statistics. With parameters traditionally being determined using experimental characterization methods in electrochemical laboratories, there is a considerable disconnect between practitioners (electrochemists) and practice (control, optimization and statistics). This also applies in the opposite direction as BMS, and therefore control engineers, are increasingly using physics-based battery models based on electrochemistry. A main goal with this review is to bridge the gap between researchers from different domains that strive to improve battery model parametrization. This is done by providing a summary of a large body of work that concerns different aspects of parameter estimation (PE) of physics-based battery models, but also a clarification of the different steps in the parametrization process, from data collection to model validation. This process, and the theory behind it, belongs to the field of *system identification* [31].

The content of the review is organized as follows. Optimization of battery model parameters as well as a background on various classes of optimization algorithms are introduced in Section 4. Information content in data and the importance of individual model parameters can be assessed using sensitivity analysis (SA), as outlined in Section 5. The concept of identifiability is treated in Section 6, along with literature that studied the identifiability of the battery model parameters. It is possible to design experiments that produce informative data, in order to improve PE. Experiment design for battery PE is featured in Section 7. In recent years, machine learning (ML) has been applied to a large variety of fields and applications. Section 8 reviews literature in which ML is used for battery PE. Finally, the importance of careful model validation, along with several available validation methods, are discussed in Section 9. Before diving into each of these topics, Section 2 provides a brief introduction to system identification and all covered steps of the parameter identification process, while Section 3 introduces the physics-based battery models, their parameters and their limitations.

## 2. Introduction to system identification

The construction of a mathematical model of a physical system is a task with many components. If the model is made based on input–output data measured on the real system, the process is referred to as

system identification [31]. Typical steps in the system identification process include selection of model structure, design of experiments, data collection, optimization of parameters and model validation [32]. This section will briefly introduce concepts that are relevant for understanding the literature on battery model parametrization, starting with the model formulation.

All models can be positioned on a gray scale from white to black, where *white-box* models are based on physical modeling from first principles whereas *black-box* models simply are flexible functions without physical meaning [33]. A model that is based on physical insight but has some parameters that are identified through fitting of experimental input–output data is called *gray-box* [34]. The battery models considered in this review (Section 3) are generally gray-box models. Their structures are based on knowledge about the electrochemical and mechanical processes that happen inside battery cells, but their parameters are obtained from a combination of physical insight and parameter fitting.

The DFN model described in Section 3 consists of a system of PDAEs that can be reduced to a set of differential algebraic equations by model reduction or by discretization of the spatial variable [10,35]. It is often useful to express differential equations as a *dynamical system* that describes how the states of the system evolve with time, given the present states as well as the applied input. In the context of battery modeling, the states are typically the lithium concentrations in the electrodes and Li-ion concentrations in the electrolyte. The internal potentials in their turn can be seen as algebraic variables that are determined from the states and the input. The input would be the applied current and the output the cell voltage, since these are measurable on the real cell. The continuous dynamical system representation of the differential algebraic equations becomes:

$$\dot{\mathbf{x}}(t) = \mathbf{f}(\mathbf{x}(t), \mathbf{z}(t), \mathbf{u}(t), \boldsymbol{\theta}) \tag{1a}$$

$$\mathbf{z}(t) = \mathbf{g}(\mathbf{x}(t), \mathbf{z}(t), \mathbf{u}(t), \boldsymbol{\theta}) \tag{1b}$$

$$\mathbf{y}(t) = \mathbf{h}(\mathbf{x}(t), \mathbf{z}(t), \boldsymbol{\theta}) \tag{1c}$$

where $t$ denotes the time, $\mathbf{x}(t) \in \mathbb{R}^{N_x}$ are the state variables, $\mathbf{z}(t) \in \mathbb{R}^{N_z}$ the algebraic variables, $\mathbf{u}(t) \in \mathbb{R}^{N_u}$ the inputs and $\mathbf{y}(t) \in \mathbb{R}^{N_y}$ the outputs. The vector $\boldsymbol{\theta} \in \mathbb{R}^{N_\theta}$ contains all the model parameters. This notation is kept throughout the paper, from here on assuming that $N_y = N_u = 1$. In practice, experimental data will not be continuous but sampled. It is therefore often useful to approximate Eq. (1) as a discrete dynamical system:

$$\mathbf{x}(k+1) = \mathbf{f}_d(\mathbf{x}(k), \mathbf{z}(k), u(k), \boldsymbol{\theta}) \tag{2a}$$

$$\mathbf{z}(k) = \mathbf{g}(\mathbf{x}(k), \mathbf{z}(k), u(k), \boldsymbol{\theta}) \tag{2b}$$

$$y(k) = h(\mathbf{x}(k), \mathbf{z}(k), \boldsymbol{\theta}) \tag{2c}$$

where $k$ is the sampling instant. The discrete system can be obtained e.g. by finite-difference approximation of the time derivatives [10]. In reality, no model can fully match experimentally measured data nor perfectly describe all the processes of a real system. Unknown disturbing signals inside the system (*process noise*) and measurement noise affect the observed output. Deviations between a model and reality, despite perfect parametrization and without noise, are called *structural errors* [32].

Given a model and observational data, it is possible to estimate the unknown parameters. A rule for how to do this is called an *estimator*. It is customary to formulate the estimator as an optimization problem in the unknown parameters

$$\hat{\boldsymbol{\theta}} = \arg\min_{\boldsymbol{\theta}} F(\boldsymbol{\theta}; \mathbf{y}), \tag{3}$$

where $F$ is a *cost function* and $\mathbf{y} \in \mathbb{R}^N$ a vector that contains the measured outputs for $N$ time steps [36]. The cost function should penalize errors between the measurements and the output predicted by the model Eq. (2), but it can also be used to discourage deviations between the estimated parameters and prior assumptions on these. A common choice is the least-squares-estimator, given by

$$\hat{\boldsymbol{\theta}}_{LS} = \arg\min_{\boldsymbol{\theta}} \sum_{k=1}^{N} (y(k) - \hat{y}(k, \boldsymbol{\theta}))^2 \quad . \tag{4}$$

Since the battery models typically are nonlinear in the parameters, $\hat{\boldsymbol{\theta}}_{LS}$ is known as the nonlinear least-squares estimator. The performance of an estimator $\hat{\boldsymbol{\theta}}$ can be separated into *accuracy* and *precision* [37]. Accuracy describes the deviation of the expected estimator $E[\hat{\boldsymbol{\theta}}]$ from the true parameter vector $\boldsymbol{\theta}^*$, and is defined by the *bias*

$$\beta(\hat{\boldsymbol{\theta}}) = E[\hat{\boldsymbol{\theta}}] - \boldsymbol{\theta}^*. \tag{5}$$

A non-linear least-squares estimator is generally biased for a finite sample [32,37,38]. In the presence of noise in the data, Eq. (4) would therefore on average not yield the true parameter vector. Precision is a measure of the estimator variability, arising from random noise [37]. Together, they constitute the *mean squared error* (MSE)

$$MSE(\hat{\boldsymbol{\theta}}) = E\left[\|\hat{\boldsymbol{\theta}} - \boldsymbol{\theta}^*\|^2\right] = \|\beta(\hat{\boldsymbol{\theta}})\|^2 + E[\|\hat{\boldsymbol{\theta}} - E[\hat{\boldsymbol{\theta}}]\|^2] \quad , \tag{6}$$

where the last term is the variance of the estimator. In reality, the model does not fully capture the true system. Structural errors will lead to a bias between the optimally parametrized model and the true system and likely also a bias in the estimation of parameters that does have a physical true value. A simple model with too few parameters or relations tends to have a high bias whereas a complex model with too many dependencies has high variance. A good model therefore is not necessarily unbiased, but has a good balance of bias and variance, which manifests as a low MSE [32].

Problem Eq. (3) can be solved using a variety of optimization methods, depending on the properties of $F$. One important distinction is between convex cost functions, for which any local minimum is also globally optimal, and non-convex cost functions which may have multiple local minima of varying quality (and also local maxima and saddle points). In the context of battery modeling, most PE problems are non-convex. For these problems, some algorithms can only guarantee convergence to a stationary point, while others attempt to find the globally optimal parameters. Algorithms that only search for local optima tend to converge quickly but may be sensitive to initialization, while algorithms that search for the global optimum may have very long running times. Generally speaking, the more information the optimization algorithm has about $F$, the faster it can find a local optima. Some optimization algorithms use first and second-order derivatives of the cost function, while others only require function evaluations. Algorithms and methodologies for optimization of battery model parameters are further covered in Section 4.

Regardless of optimization method, not all problems can be solved. A parameter $\theta$ of model $K$ is globally *identifiable* if the following condition holds:

$$K(t, \theta) = K(t, \theta^*) \Rightarrow \theta = \theta^* \quad , \tag{7}$$

which implies that there should only exist one unique solution [39]. Due to model structure, there can be parameters that take on multiple or infinite different values but yield the same result. Unidentifiability can also be of practical nature. Practical unidentifiability results from lack of information in the experimental data due to the type of dynamics it contains or the presence of noise. Identifiability is a measure of model validity since only an estimate of an identifiable parameter can be trusted for all input signals. Identifiability is treated in Section 6.

The information contained in data about a parameter can be assessed by analyzing its sensitivity, see Section 5. Parameter sensitivity is best understood as the impact a parameter has on the model output. Changing a highly sensitive parameter will result in large model output variations, whereas changes in a less sensitive parameter will have less effect. Hence, an incorrect sensitive parameter leads to large errors in the output while an incorrect insensitive parameter will produce

smaller errors. SA is therefore a useful tool to determine which parameters to identify from data and which to assume from literature values or intuition. The sensitivity depends on the parameter values, the model structure and the applied input signal [40]. An input signal that makes a parameter sensitive and possible to distinguish from other parameters is said to be informative about the parameter in question.

The input signal's effect on the sensitivity of the parameters provides an opportunity to improve the estimation accuracy by altering the input. The field concerned with design of experiments for parameter identification is called Optimal Experiment Design (OED) or Design of Experiments. The main idea is to algorithmically relate the parameter sensitivities to experiment input factors, and then optimize the input factors to achieve maximum parameter identifiability [41]. Input factors that can be optimized are sampling time, test duration, initial conditions, constant control variables and time-varying control variables [42]. In the case of battery model experiment design, the initial conditions could be the starting SOC, the constant control variable the ambient temperature and the time varying control variable the current input. Experiment design for battery model parametrization is covered in Section 7.

An important, but sometimes overlooked, part of the modeling process is the validation. This step should reveal whether the model can predict the true system output sufficiently well for its intended purpose [31]. Deviations between the model output and experimental measurements do not only derive from poorly estimated parameters, but also from measurement errors, numerical errors in the model solution algorithm, and a general inability of the model to capture the true system dynamics [43]. Although it is important that the parametrized model is able to produce accurate predictions of the fitting data, it is essential that it is also able to extrapolate beyond the data which was used for PE. The latter is motivated by the fact that a perfect match to experimental observations can be achieved by adding enough parameters and dependencies to a model. However, an over-fitted model will not yield comparable results on other data sets because it is not modeling the true behavior correctly. It is recommended to test a model in a wide range of operating conditions outside its fitting data (*cross-validation*) since validation on the fitting data (*auto-validation*) cannot ensure that the model is generally valid [31]. Methods for model validation are further treated in Section 9.

Fig. 1 illustrates how the concepts introduced in this section can be implemented in the PE process. As shown in many examples throughout the review, these analyses however have multiple uses. Therefore, the figure should be seen as a suggested systematic approach rather than something to follow in all situations. A modeling study starts with formulating or selecting a model structure that can capture the processes that are of interest. Each model contains a set of parameters. The higher the dimension of parameter space, the more challenging the PE task. A second step in the process is often to reduce the number of unknown parameters. Structural IA can reveal parameters that cannot be identified from any data. Subsequently, a SA using data representative of the intended model application can show which parameters are going to be sensitive, and thus important to accurately estimate. Once the dimension of parameter space is reduced, the goal is to reduce the uncertainty about the parameters. The green segment of the chart illustrates the process of going from only knowing reasonable parameter bounds to obtaining estimated optimal values as well as measures of their performance. The values of the parameters are optimized so that model simulations resemble experimental measurements. The experiments used for this fit are designed in order to increase the identifiability of the unknown parameters. Sometimes, this is a step-wise and/or iterative process. Practical identifiability analysis and other validation methods conclude this procedure in order for the modeler to know how much confidence to put in the final, parametrized model. The following sections elucidate the different parts of the PE process and summarize literature regarding these. The different components in the figure are not in the exact order the paper is structured as many concepts build on one another.

## 3. Battery modeling

### 3.1. Physics-based battery modeling

The parametrization techniques laid out in this paper can apply to all mathematical models. Since the reviewed literature is mainly based on physics-based Li-ion battery models, this section will discuss the most commonly used model, specifically the DFN model. The rich body of work covering mathematical equations for Li-ion batteries can be largely traced back to two publications by Doyle, Fuller and Newman from 1993/94 [18,19]. The DFN model describes one-dimensional porous electrodes at the scale of $\sim$ 100 μm, coupled with another dimension for the active material particles at the scale of $\sim$ 1 μm. Thus, the model of the electrodes is formulated on the product space of two 1D domains and is therefore often referred to as pseudo-2D (P2D) model. In the following sections, we will use the term 'DFN model', which carries identical definitions and assumptions as the term 'P2D model'. The geometry includes the negative electrode, separator and positive electrode; current collectors are at both boundaries and the charge transfer reactions are distributed along the electrode depth $x$. In the spherical particle domain, intercalated lithium diffuses along the radial dimension $r$. The two domains are illustrated in Fig. 2.

The underlying structure of the model is based upon porous electrode theory, including charge and mass balances in the electrolyte and the electrode phases and charge transfer kinetics. The governing equations for the DFN model are summarized in Table 1. According to porous electrode theory [44], the porous electrodes are a superposition of three phases, i.e. electrolyte, electrochemically active material, and inactive materials like conductive filler and binder. Each phase has its own volume fraction. Sometimes, the porous structures are treated explicitly [45]. Concentrated solution theory describes the transport of ionic species in the electrolyte phase by relating the driving force (the electrochemical potential gradient) to the mass flux [46]. This, together with a source term, is then put into the mass balance equation to describe concentration change, as in Eq. (8). Charge balance describes the amount of current passed from the solid active electrode material to the electrolyte. Ohm's law is used in the electrode as described in Eq. (12). In the electrolyte, the transport equation takes migration and diffusion into account, as described in (15). Charge transfer kinetics such as Butler–Volmer equation in Eq. (19) is used to couple the electrode domain with the particle domain. It includes the relationship between an electrochemical rate constant or exchange current density given in Eq. (20) and the potential difference between the electrode and electrolyte given in Eq. (21). Solid-state lithium (de)intercalation along $r$ is often described by Fickian diffusion, as in Eq. (22).

A common simplification is the SPM [20,21], where each electrode is reduced to a single spherical particle, as shown in Fig. 2. It considers a uniform current distribution in the entire electrode and neglects electrolyte transport limitations. Expansions on this simplification aim to include electrolyte effects while keeping the computational advantages [47], this is termed SPMe in the following sections. Similar to the DFN model, Fick's second law describes the lithium concentration in the (de)intercalated solid active particle and charge transfer kinetics such as Butler–Volmer equation describes the electrochemical reaction on the solid particle/electrolyte surface.

Many authors [48–52] couple the electrochemical model outlined above with a thermal model. One application is to facilitate thermal management strategies in situations when thermal issues may cause safety concern, capacity or power fade, or poor performance due to low temperature etc. Thus, accurate estimation of temperature evolution, e.g. for a proposed charging strategy in an EV, is an essential component of control oriented models. Surface temperature, next to the cell voltage, is a battery state commonly measured and readily available in BMS. To properly model the battery thermal conditions, it is necessary to include temperature dependency of certain model parameters (see Section 3.2).

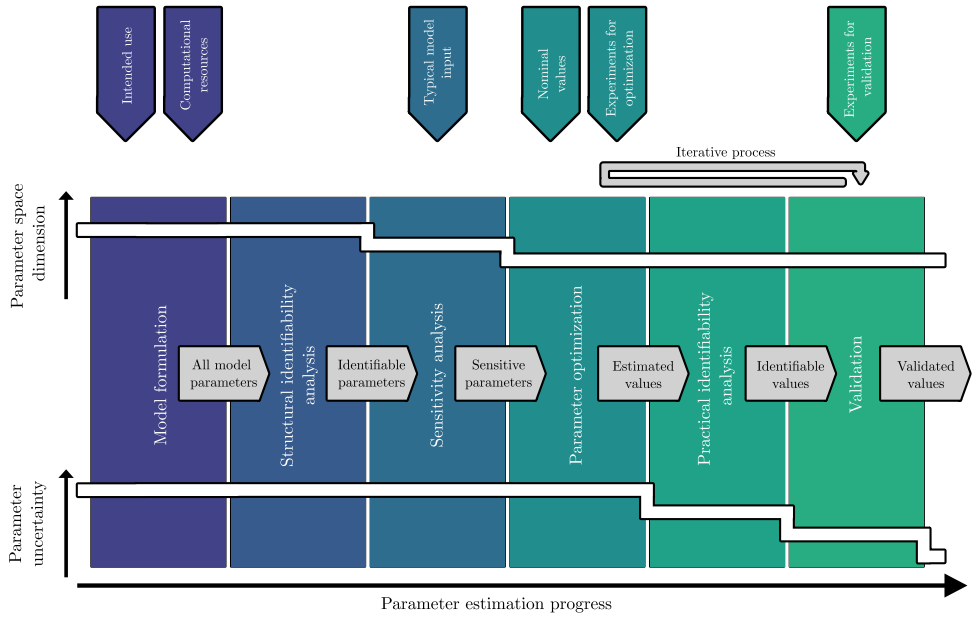


**Fig. 1.** Components of a PE study.

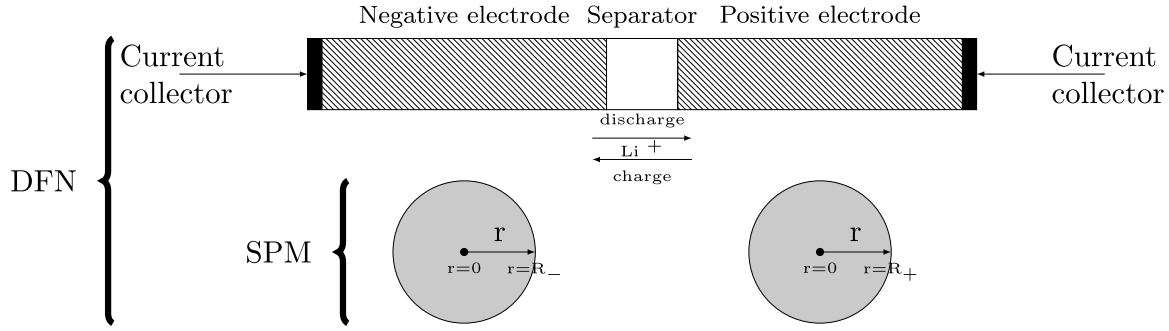


**Fig. 2.** Schematic of the DFN model with two porous electrodes and spherical active material particles and the SPM simplification consisting only of two particles.

As these models, both thermal and electrochemical, are established and stated in numerous publications we refer interested readers to the references above for a more in-depth discussion. Table 1 describes the governing equations for the DFN model. The given equations Eq. (8)–(23) do not cover a thermal model, but it nevertheless already contains more than 30 parameters. The implementation or coupling with a thermal model requires the formulation of the energy balance equation. The PDAEs are solved numerically using different tools. A widely used numerical implementation is found in COMSOL Multiphysics [53]. Packages are also available in Matlab [35] and Python [54].

### 3.2. Model parameters

Many of the parameters in Table 1, such as diffusion coefficients $D_{\pm}$ and reaction rate constants $k_{\pm}$, may strongly depend on SOC, temperature $T$, SOH, or the spatial coordinate $x$ such that they can usually not simply be described by a single value. SOC- and $T$-dependent parameters are generally identified with destructive or non-destructive electrochemical and analytical measurements. Even when disregarding such dependencies, the majority of these parameters prove difficult to be determined from measurements and are thus commonly obtained by PE. As cells age, these parameters change considerably. However, investigation of parameters' SOH-dependency is remarkably arduous. A possible approach is to obtain them exclusively with PE [55]. Occasionally, lumped parameters with SOC-, $T$- and SOH-dependency are investigated using reduced order model (ROM) [56,57]. Model parameters for the DFN model and their dependencies are listed in Table 2.

In the following illustrative example, we highlight one particularly common formulation for the particle domain's parameters and the challenge that comes with it. Based on the assumption of Fick's second law, each electrode's particle domain can be characterized by a particle radius $R_{\pm}$ and $D_{\pm}$, as in Eq. (22), (23). The spherical particle radii are often set to a single value, implying perfectly homogeneous electrodes. However, depending on the electrode chemistry, real electrodes often contain non-spherical primary and secondary particles with size distributions varying by one order of magnitude. Together with $D_{\pm}$ they form a solid lithium diffusion time constant $t_{\pm} = \frac{R_{\pm}^2}{D_{\pm}}$ [58]. It is this characteristic time constant that can be distinguished from electrochemical experiments. This strong interdependence means $R_{\pm}$ and $D_{\pm}$ are only identifiable as a coupled time constant and not individually. In fact, since the surface area of the active material $a_{\pm}$ is commonly derived from $R_{\pm}$ and active material volume fraction $\varepsilon_{\pm}$, i.e. $a_{\pm} = \frac{3\varepsilon_{\pm}}{R_{\pm}}$ for spherical particles, $t_{\pm}$ can also be linked with $a_{\pm}$ and thus the volumetric current.

The issue with parameter interdependence and identifiability can be found for other parameter sets like porosity $\varepsilon_{e,\pm}$ and electrolyte tortuosity $\tau_{e,\pm}$, active material fraction $\varepsilon_{\pm}$ and electrode thickness $L$ etc. To address these problems, additional effort is required, e.g. experimental measurements and invasive methods (cell opening). Many authors also resort to literature or assumed values for at least one of the parameters in each coupling. This might not reflect the real

**Table 1**
Governing equations for the DFN model.

| Equations | Boundary condition | Eq. no. |
|---|---|---|
| $Li^+$ transport in electrolyte phase | | |
| $\frac{\partial \varepsilon_{e,\pm} c_e}{\partial t} + \nabla \cdot \left(-D_{e,\pm}^{eff} \nabla c_e\right) = \left(\frac{1-t_+^0}{F}\right) i_{tot}$ | $\frac{\partial c_e}{\partial x}\|_{x=0,L} = 0$ | (8), (9) |
| $D_{e,\pm}^{eff}(c_e) = D_e(c_e)\frac{\varepsilon_{e,\pm}}{\tau_{e,\pm}}$ | | (10) |
| $i_{tot} = i_{loc,\pm} a_\pm$ | | (11) |
| Charge conservation | | |
| Electrode phase: | | |
| $\nabla \cdot \left(-\sigma_\pm^{eff} \nabla \Phi_\pm\right) = -i_{tot}$ | $\Phi_-\|_{x=0} = 0 \sigma_-^{eff} \frac{\partial \Phi_-}{\partial x}\|_{x=L_-} = 0$<br>$\sigma_+^{eff} \frac{\partial \Phi_+}{\partial x}\|_{x=L_-+L_s} = 0 \sigma_+^{eff} \frac{\partial \Phi_+}{\partial x}\|_{x=L} = -\frac{I_{cell}}{A_{cell}}$ | (12), (13) |
| $\sigma_\pm^{eff} = \sigma_\pm \frac{\varepsilon_\pm}{\tau_\pm}$ | | (14) |
| Electrolyte phase: | | |
| $\nabla \cdot \left(-\kappa_\pm^{eff} \nabla \Phi_e\right) + \nabla \cdot \left(\kappa_{D,\pm}^{eff} \nabla \ln c_e\right) = i_{tot}$ | $\frac{\partial \Phi_e}{\partial x}\|_{x=0,L} = 0$<br>$\frac{\partial c_e}{\partial x}\|_{x=0,L} = 0$ | (15), (16) |
| $\kappa_\pm^{eff}(c_e) = \kappa(c_e)\frac{\varepsilon_{e,\pm}}{\tau_{e,\pm}}$ | | (17) |
| $\kappa_{D,\pm}^{eff} = \frac{2RT\kappa_\pm^{eff}}{F}\left(1 + \frac{\partial \ln f_\pm}{\partial \ln c_e}\right)(1 - t_+^0)$ | | (18) |
| Charge transfer kinetics | | |
| $i_{loc,\pm} = i_{0,\pm}\left[exp\left(\frac{\alpha_{a,\pm} F}{RT}\eta_\pm\right) - exp\left(-\frac{\alpha_{c,\pm} F}{RT}\eta_\pm\right)\right]$ | | (19) |
| $i_{0,\pm} = F k_\pm (c_{max,\pm} - c_{surf,\pm})^{\alpha_{a,\pm}} (c_{surf,\pm})^{\alpha_{c,\pm}} \left(\frac{c_e}{c_{e,0}}\right)^{\alpha_{a,\pm}}$ | | (20) |
| $\eta_\pm = \Phi_\pm - \Phi_e - U_\pm(c_\pm)$ | | (21) |
| Lithium transport in particle domain | | |
| $\frac{\partial c_\pm}{\partial t} = \frac{1}{r_\pm^2}\frac{\partial}{\partial r}\left(D_\pm r_\pm^2 \frac{\partial c_\pm}{\partial r}\right)$ | $\frac{\partial c_\pm}{\partial r}\|_{r=0} = 0$<br>$D_\pm \frac{\partial c_\pm}{\partial r}\|_{r=R_\pm} = -\frac{i_{loc,\pm}}{F}$ | (22), (23) |

electrode parameter and thus result in an erroneous estimation for interdependent parameters.

While usually neglected in models, insertion and deinsertion of lithium can have a considerable impact on the lattice structure of the electrode materials through which Li-ions must be transported. In this manner, active material properties depend on state-of-lithiation (SOL) or SOC. Additionally, electrode properties depend on operating conditions such as $T$, internal battery states such as electrolyte salt concentration $c_e$ or the location in the electrode domain $x$, and manufacturing processes. As the battery ages, nearly all properties described for both the electrodes and separator may change, which can be modeled with SOH-dependent parameters. Table 2 highlights the parameters, of which their dependencies are commonly considered. These considerations emphasize the importance of accurate PE methodology and highlight how measurements often cannot be trivially translated into parameter values.

### 3.3. Electrode balancing

Any predictive capability of a physics-based model depends on accurate electrode balancing. It is an important first step because it provides the exact representation of open circuit voltage (OCV) of each electrode, which corresponds to the full cell OCV. Electrode balancing is unique to the system and cannot be obtained from literature [23]. Without appropriate balancing any parameter optimization effort is deemed futile as the erroneous half-cell stoichiometry will dominate any estimation error. In practice, the dependency between full-cell SOC and half-cell SOL is often established with electrode balancing models and voltage fitting techniques. We determine parameters like the start and end stoichiometric points of the positive and negative electrode, i.e. the parts of their respective OCVs that are used, and thus their capacities.

The obligatory input data is the full-cell OCV. OCV data can be determined using continuous pseudo-OCV [22,25] measurements at currents close to but not equal to zero. A more rigorous and exact approach measures a series of OCV points when the cell reaches equilibrium after a current pulse [22]. Half-cell OCV data can be measured with the same method. However, it requires not only cell opening and construction of laboratory cells to separate signals from positive and negative electrodes, but also a well-defined reference or counter electrode, which may often be hard to be achieved experimentally. To avoid cell opening, literature OCV data for similar single electrode materials is sometimes used. While having measurements for the specific material is advantageous, half-cell OCV data for the same electrode chemistry that is available from literature can be a reasonable compromise.

During battery operation, a full utilization of the theoretical capacities of positive and negative electrodes are often avoided [22,23,25]. Graphite, as being the most commonly used negative electrode, is usually not fully lithiated (SOL<1) at 100% SOC to prevent lithium plating [6] and not fully delithiated (SOL>0) at 0% SOC in order to avoid to copper stripping from the current collector. Positive electrodes are often not fully delithiated (SOL>0) at 100% SOC due to layer formation and structural instability. At the other end, they are not fully lithiated (SOL<1) at 0% SOC due to cell balancing with graphite being the limiting electrode. In addition, loss of lithium inventory and loss of active material due to e.g. side reactions or mechanical degradation continuously shifts the electrode balancing [62]. Detecting and quantifying these shifts is thus an important tool for SOH estimation of aging batteries [61,63,64].

### 3.4. Model limitations

An accurately represented and parametrized model can be used as a predictive tool for battery performance, dynamics and lifetime. However, the models introduced above have their limitations due to the underlying assumptions. A trivial example is that the one dimensional electrode domain cannot predict any phenomena of dimensions higher than 1D+pseudo 1D, such as geometrical inhomogeneity (particle size, porosity and tortuosity distribution) [65], non-uniform internal electrode states and non-uniform aging [66,67]. For instance, batteries show large inhomogeneity in current distribution under high charge/discharge rates. During aging, they may show uneven changes in morphology and topology. Consequently electrochemical and analytical characterization methods, which are usually based on a small sample cell, can only give accurate parameters if electrode properties are entirely uniform. In this sense, fitting SPM and/or DFN model to such data can only provide effective properties, i.e. average or bulk values and mask any effects of non-uniform distribution.

**Table 2**
DFN Model parameters and their dependencies on SOC, position in the electrode $x$, electrolyte salt concentration $c_e$, temperature $T$ and SOH.

| Symbol | Description | Dependencies | References |
|---|---|---|---|
| Particle domain | | | |
| $D_{\pm}$ | Solid diffusion coefficient | $T$ | [24,25,56] |
| | | SOC | [22,24,25,56] |
| | | SOH | [55,59] |
| $R_{\pm}$ | Particle radius | $x$, SOH | |
| Electrode domain | | | |
| Electrolyte properties | | | |
| $D_e$ | Electrolyte diffusion coefficient | $T$ | [60] |
| | | $c_e$ | [60] |
| | | SOH | [59] |
| $\kappa$ | Ionic conductivity | $T$ | [24,25,60] |
| | | $c_e$ | [24,25,60] |
| $t_+^0$ | Cationic transference number | $T$ | [24,25,60] |
| | | $c_e$ | [60] |
| $1+\frac{\partial f_{\pm}}{\partial \ln c_e}$ | Activity coefficient | $T$ | [24,25,60] |
| | | $c_e$ | [60] |
| $c_{e,init}$ | Initial electrolyte $Li^+$ concentration | – | |
| $\tau_{e,\pm}$ | Electrolyte tortuosity | $x$, SOH | |
| $\epsilon_{e,\pm}$ | Electrolyte volume fraction | $x$ | |
| | | SOH | [59] |
| Active material properties | | | |
| $\sigma_{\pm}$ | Electronic conductivity | – | |
| $\tau_{\pm}$ | Electrode tortuosity | $x$, SOH | |
| $k_{\pm}$ | Reaction rate constant | $T$ | [22,24,25,56] |
| | | SOC | [24,25,56] |
| $\alpha_{a,\pm}, \alpha_{c,\pm}$ | Anodic/cathodic charge transfer coefficient | – | |
| $U_{\pm}$ | Open circuit potential (OCP) | $T$ | [56] |
| | | SOC | [56] |
| | | SOH | |
| $\epsilon_{\pm}$ | Active material volume fraction | $x$ | |
| | | SOH | [59,61] |
| $L_{\pm}$ | Electrode thickness | SOH | [55] |
| $a_{\pm}$ | Volume specific electrode area | $T$ | [56] |
| | | SOC | [56] |
| | | SOH | [55] |
| $c_{max,\pm}$ | Maximum lithium concentration in active material | SOH | [55] |
| $c_{init,\pm}$ | Initial lithium concentration in active material | SOH | [59] |
| Separator domain | | | |
| $\epsilon_s$ | Separator porosity | SOH | |
| $\tau_s$ | Separator tortuosity | SOH | |
| $L_s$ | Separator thickness | SOH | |

Model limitations may also stem from an inherently incomplete model where e.g. thermal effects, hysteresis, mechanical effects, side reactions, aging, influence of additives such as conductive carbon support and binders etc. are not considered. For example, during battery aging new layers can grow on the active material which would end up being bulked into reaction rate constants, diffusion coefficients or electrolyte conductivity during parameter optimization if not treated explicitly. Model accuracy will drastically deteriorate during aging if side reactions and mechanical degradation are not addressed [55]. Nonetheless, additional mechanisms need to be addressed carefully with realistic chemical and physical representation, since an increase in degree of freedom may compromise parameter accuracy, sensitivity and identifiability.

These problems can be targeted by increasing model dimensionality [45,68], considering necessary mechanisms or including physical aging models. A multitude of "expansions" or variations of the DFN model have evolved over the years. For example, 3D microstructural models can be used to examine non-uniformities in current distribution, SOL, temperature and discharge capacity [69,70]. These, however, entail additional parameters and come at the expense of increased computational cost. One should be aware that a more complex model may sometimes result in an over-fitted model, which should be avoided.

## 4. Parameter optimization

Extraction of battery model parameters from experimental data involves fitting the parameters so that model predictions match the measured signals. This is done by minimizing a cost function (also known as *objective function*) designed to penalize deviations between the model response and measurements. The most frequently used cost function in the battery literature is the sum of squared deviations between the measured and predicted cell voltage, as in the least-squares Eq. (4). In general, although not common in battery parametrization research, modifications of the least-squares objective can be made in order to take prior information about the parameters or the experimental data into account [71]. If structural errors are expected to be significant, the cost function can be weighted such that smaller errors are obtained where good performance is needed while larger errors manifest where deviations can be accepted [32]. Under the assumption that the prediction error is normally distributed, the least-squares estimator is equivalent to a *maximum likelihood* estimator [72]. In cases when it is not, the least-squares cost (4) is only motivated from a practical, and not statistical, standpoint [32,72]. For readers interested in the statistical theory of parameter estimators, we refer to e.g. [72].

Optimization problems can be classified based on the properties of their cost function (and possible constraints), as mentioned in Section 2. The main distinction in the modern optimization literature is between convex and non-convex problems. Optimization of battery model parameters typically results in non-convex problems, characterized by multiple local optima and/or saddle points with solutions of different cost [73]. Different optimization methods will work well for some problems but be less successful for others.

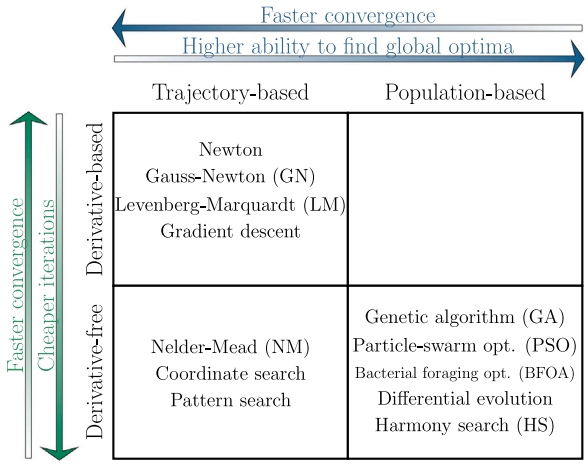


**Fig. 3.** Classification of a subset of optimization methods that has been used for battery PE. Methods that are both derivative-based and population-based exist in other non-battery literature (see for example [77]) but are not represented in this review.

Fig. 3 shows the optimization methods that have been used for physics-based battery model parametrization and Table 3 summarizes the reviewed literature. The methods are discussed in more detail in the remainder of this section. We divide them into derivative-based methods that employ first- and sometimes second-order derivatives of the cost function, and derivative-free methods that only rely on function evaluations. We will also distinguish between trajectory-based and population-based methods. The former updates a single candidate solution every iteration, while the latter uses multiple alternative points with separate trajectories.

In many battery applications, the time and computational resources that can be spent on parameter estimation are limited. Therefore, the performance of a method is often evaluated both based on the final cost function value and on optimization time. Two factors determine the total optimization time: the time it takes to perform one iteration of an algorithm and the number of iterations needed for convergence [74]. The former strongly depends on the number of required model evaluations per iteration and the time each of these take. The latter is affected by the amount of information about the cost function that is available to the algorithm: the more information, the faster the convergence. For global algorithms, like the population-based methods in Fig. 3, there is a trade-off between optimization time and optimality of the solution [74]. Many optimization methods are readily available in Matlab's Optimization Toolbox and COMSOL's Optimization Module. Examples of open source alternatives are SciPy [75] and PyMoo [76].

### 4.1. Derivative-based optimization

Many classical optimization algorithms belong to the class of derivative-based methods. Their basic principle is intuitive to understand: starting at some point in parameter space, one iteratively takes steps in a direction that decreases the cost function using information about its gradient and sometimes curvature. The curvature of the cost function is described by the *Hessian* matrix of partial second derivatives. Extreme points are characterized by zero gradient vector and positive-semidefinite (minimum) or negative-semidefinite (maximum) Hessian [95]. All *line-search* methods follow the same procedure as in Algorithm 1 [96]. In each iteration $i$, a step direction, $\mathbf{p}^{(i)}$, in parameter space is computed based on some approximation of the cost function. Different step directions are introduced throughout the remainder of this section. Second, a step size, $\alpha^{(i)}$ is calculated. If the step size is too small, the convergence is very slow whereas if it is too big, the algorithm might diverge. Third, the parameter estimate is updated by taking a step $\alpha^{(i)}\mathbf{p}^{(i)}$, in the computed direction.

**Algorithm 1** Gradient-based optimization with line-search.

**while** Convergence = false **do**
1. Compute step direction, $\mathbf{p}^{(i)}$
2. Compute step size, $\alpha^{(i)}$
3. Update parameter estimate: $\hat{\boldsymbol{\theta}}^{(i+1)} = \hat{\boldsymbol{\theta}}^{(i)} + \alpha^{(i)}\mathbf{p}^{(i)}$

**end while**

In *trust-region* methods, the step size represents a region around the current iterate in which we trust the approximation of the cost function to be accurate [96]. The step direction and step size are determined simultaneously to minimize the approximation inside the trust region.

An intuitive choice of step direction is the negative gradient, which represents the direction of steepest slope and thus the fastest cost reduction. The gradient descent method guarantees that some stationary point is found, but has the disadvantage of slow convergence and sensitivity to numerical ill-conditioning [97]. Another well-known line-search algorithm is Newton's method, in which the objective function is approximated by a second order Taylor expansion around the iterate. Using second-order information is advantageous because it increases the convergence rate and improves the robustness towards ill-conditioned problems [96]. However, for large problems, significant computations and memory are required to evaluate and store the Hessian [97]. *Quasi-Newton* methods make use of Hessian approximations to reduce the computational burden while maintaining high convergence rate [96]. The Gauss–Newton (GN) algorithm for optimization of the least-squares problem Eq. (4) avoids the use of the Hessian altogether by performing a first-order approximation of the output. The convergence of the GN method depends on the initial guess of the parameters as well as the response of the model to explored parameter sets. Close to optima, the convergence can be rapid, but there is no guarantee that the algorithm will converge [96].

The Levenberg–Marquardt (LM) method is an interpolation between GN and gradient descent, that can take advantage of the strengths of both methods. In recent years, due to the increasing use of the DFN model, LM has been employed by many researchers as an efficient non-linear least-square estimation algorithm for optimization of battery parameters [80,83,92]. The built-in LM algorithm in commercial software like COMSOL Multiphysics also increases its usage in extracting battery parameters from experimental data. The step direction of the LM algorithm is

$$\mathbf{p}^{(i)} = [\mathbf{J}(\boldsymbol{\theta}^{(i)})^T\mathbf{J}(\boldsymbol{\theta}^{(i)}) + \lambda_{LM}\mathbf{I}]^{-1}\mathbf{J}(\boldsymbol{\theta}^{(i)})^T(\mathbf{y} - \hat{\mathbf{y}}(\boldsymbol{\theta}^{(i)})) \quad , \tag{24}$$

where $\mathbf{J}$ is the *Jacobian* of the output as defined by

$$\mathbf{J}_{k,j} = \frac{\partial \hat{y}(k,\boldsymbol{\theta})}{\partial \theta_j}\Big|_{\boldsymbol{\theta}=\boldsymbol{\theta}^{(i)}} \quad , \tag{25}$$

$\mathbf{I}$ is the identity matrix and $\lambda_{LM}$ is a parameter that controls the step size [96]. For small $\lambda_{LM}$, the direction will be close to a GN step and for large $\lambda_{LM}$, the parameter update will be close to a gradient descent step. The battery parameters often have a large spread in magnitude, which can make the problem badly scaled and cause issues in setting an appropriate step size in the algorithm. One solution is to replace the identity matrix in Eq. (24) with a positive diagonal matrix $\mathbf{D}$ with entries that gets updated throughout the optimization [96].

One of the earliest papers using LM for battery physics-based modeling is from Santhanagopalan et al. [92] in 2007, where parameters were estimated from charge–discharge curves. Deng et al. [80] studied the possibility of using LM to optimize parameters of a ROM in a BMS. In their paper, a set of nine parameters were identified from pulse test and urban dynanometer drive cycles. Jin et al. [83] used LM with the DFN model to extract thermodynamic and kinetic parameters from measured discharge curves as well as dynamic profiles. A root-mean-square-error (RMSE) of less than 16 mV between the model predictions and experimental data was reported from their validation, however

**Table 3**
A summary of literature on battery model parameter optimization, including which type of model and which parameters were considered, which method was used as well as some performance measure of the results. Data produced by the model itself is referred to as synthetic data whereas real data is measured on a battery.

| Author | Model | Method | Optimized parameters | Performance aspect |
|---|---|---|---|---|
| Bi and Choe, 2018 [78] | DFN | GA | eight parameters | Absolute error < 12 mV (real data) |
| Chen et al. 2019 [79] | SPM | GA | $D_+$, $D_-$, $\varepsilon_{e,+}$, $\varepsilon_{e,-}$, $\varepsilon_{e,s}$, $\varepsilon_-$, $\varepsilon_+$ | Error: 0–56 mV, Relative voltage error: 0–0.7% (real data) |
| Chun et al. 2019 [51] | DFN+ thermal | HS | 17 parameters | Average error < 2.5 mV, validation on fitting set (real data) |
| Deng et al. 2017 [80] | SPM | LM | nine parameters | Mean error: 9.3–10.5 mV (synthetic data), relative parameter errors <20% |
| Fan, 2020 [81] | SPMe | PSO | 26 parameters in two steps | RMSE: 12.8–18.26 mV (real data) |
| Forman et al. 2012 [82] | DFN | GA | 17 parameters + 71 function coefficients | 90th percentile error: 50.5 mV (real data) |
| Jin et al. 2018 [83] | DFN | LM | $R_\pm$, $\sigma_+$, $D_e$, $D_+$, $R_{film}$, OCP coefficients | RMSE: 5.6–15.5 mV (real data) |
| Jokar et al. 2016 [84] | SPMe | GA | $D_+$, $D_-$, $k_+$, $k_-$, $a_+$, $a_-$, $c_{init,+}$, $c_{init,-}$ | Relative parameter errors: ≈0%–37% (synthetic data) |
| Li et al. 2016 [85] | DFN | GA | 21 parameters in two groups | Average error: 6.4–12.9 mV (synthetic data). Duration: <10 h. |
| Ma et al. 2016 [86] | SPM | BFOA | $D_+$, $D_-$, $k_+$, $k_-$, $a_+$, $a_-$ | Error: within 18–80 mV (real data). |
| Masoudi et al. 2015 [73] | DFN | Homotopy | $\epsilon_s$, $t_+$, $\sigma_-$, $c_{e,0}$ | Relative voltage error: within 0.04% (synthetic data). |
| Pang et al. 2019 [87] | SPMe | GA | eight parameters | RMSE < 2% voltage and SOC (real data) |
| Qi et al. 2017 [88] | SPM | GA | $D_+$, $D_-$, $k_+$, $k_-$, $R_+$, $R_-$, $\varepsilon_{e,+}$, $\varepsilon_{e,-}$, 21 OCP coefficients | Duration: <10 h |
| Rahman et al. 2016 [89] | DFN | PSO | $D_+$, $D_-$, $k_+$, $k_-$ | Graphical (real data) |
| Rajabloo et al. 2017 [90] | SPMe | GA | $D_+$, $D_-$, $k_+$, $k_-$ $a_+$, $a_-$, $c_{init,+}$, $c_{init,-}$ | RMSE: 1.6–100 mV (real data) |
| Ramadesigan et al. 2011 [59] | DFN | GN | $D_+$, $D_-$, $k_+$, $k_-$, $D_e$ | Graphical (real data) |
| Reddy et al. 2019 [91] | DFN | Hybrid algorithm | 14 parameters + 30 OCP coefficients | RMSE: < 10 mV (real data). Duration: <14 h |
| Santhanagopalan et al. 2007 [92] | SPM+ DFN | LM | $D_+$, $k_+$, $k_-$, $c_{init,+}$, $c_{init,-}$ | Graphical (real data) |
| Scharrer et al. 2013 [93] | DFN | Gradient + Space mapping | $k_+$, $c_{init,+}$, $\alpha$ | Graphical (synthetic data) |
| Shen and Li, 2017 [94] | Electrical | PSO-LM | seven parameters | Graphical (real data) |
| Zhang et al. 2013 [50] | DFN+ thermal | GA | 27 parameters | Error: <25.4 mV (real data). Duration: 22.3 h. |

they noted that the identified parameters did not change a lot from their initial guesses.

Fig. 4(a) shows an example of a cost function with multiple local optima as well as a hypothetical trajectory of a gradient-based optimization algorithm. The gradient-based algorithms discussed in this section are local methods, meaning that they converge to a local optimum that may or may not be globally optimal in non-convex problems. To increase the robustness against local minima in gradient-based methods, a homotopy transformation was used by Masoudi et al. [73] to estimate four of the DFN model parameters. The purpose of the homotopy transformation was to smoothen the objective function so that a simple gradient descent algorithm could find a global minimum. The impact of the transformation was gradually reduced throughout the optimization procedure until the true objective function was being optimized close to the global minima. By mapping out the cost function in a two-parameter identification scenario, they showed that many local minimas were present but that the proposed approach managed to find a parameter set close to the global optima. However, they noted that the efficiency of the approach diminished as the number of unknown parameters increased.

When analytical derivatives are not available, as is often the case for battery models, they can be approximated by finite differences. The computed model output may contain numerical noise and result in erroneous gradients if the noise dominates the finite difference step [96]. Finite differences can also be cumbersome and costly to compute for complex models. Scharrer and Watzenig [93] used a space mapping technique in which a coarse model was constructed by linearizing the non-linear PDAEs of the DFN model through a Taylor expansion around some reference parameter set. A mapping function between the coarse model parameters and the original model parameters was assumed and a surrogate optimization problem obtained. By doing this, they reduced the computational cost required to optimize their chosen set of parameters compared to a gradient-based approach with finite differences. However, they noted that the method resulted in increased numerical instabilities.

### 4.2. Derivative-free optimization

If gradients are not readily available, and gradient approximation is too costly or unreliable, derivative-free methods can be useful since they iterate through parameter space without the use of gradient information. The derivative-free methods are, however, less developed than their derivative-based counterparts and less effective in implementing constraints [96]. Population-based algorithms are typically derivative-free and can be employed when the goal is to find the global optimum of a non-convex cost function.

#### 4.2.1. Trajectory-based derivative-free methods

The basis for many derivative-free methods is to use interpolation to construct approximations of the objective function, similar to how Taylor expansion is used to make the approximation in derivative-based methods. Nelder–Mead (NM), also called the downhill simplex method, is a popular derivative-free method. In the battery literature, NM and a similar method named COBYLA have been implemented for the purpose of cell design optimization, e.g. optimizing cell thickness, porosity, particle sizes etc. with energy density and/or power density as the objective [98,99]. A simplex is a shape with $N + 1$ edges in an $N$ dimensional space (for example, a triangle in a 2D-space), see Fig. 4(b). The simplex is updated iteratively, by replacing the corner with the highest objective function by a point in parameter space that has a lower value. The changing simplex produces a trajectory through parameter space. It should be noted that NM is a local method and not immune towards local optima. The interested reader is referred to [96] for a thorough description of derivative-free trajectory-based methods.

#### 4.2.2. Population-based derivative-free methods

Because of their ability to search for the global optimum, derivative-free optimization based on *metaheuristic* algorithms have been explored for battery parameter identification in recent years. This class of algorithms include a number of rather diverse techniques, many of which

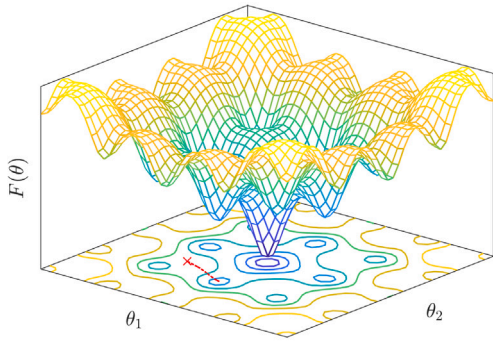


(a) If a gradient-based optimization algorithm is initialized in the point marked with a cross, it will converge to one of the local optima.

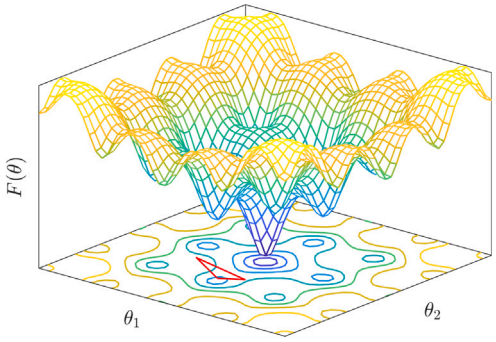


(b) The NM algorithm makes use of a simplex, and iterates towards an optima using interpolations.

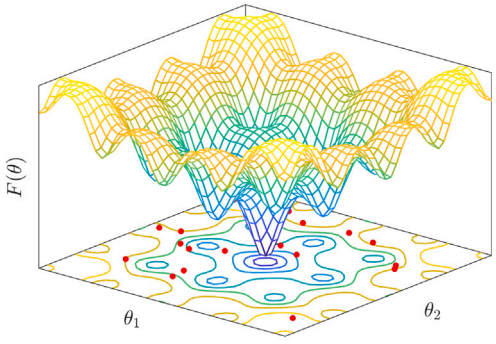


(c) In population-based metaheuristic algorithms, multiple candidate solutions are generated throughout parameter space. The solution points interact with each other in the search for the global optima.

**Fig. 4.** An example of a non-convex cost function in a 2-dimensional parameter space.

are inspired by phenomena occurring in nature. They use a population of candidate solutions that move through parameter space, often while interacting with each other. This is illustrated in Fig. 4(c). A *heuristic* is an absolute or approximated measure of a candidate's potential to evolve into the globally optimal solution [74]. It is different from the cost function, that just measures the quality of a particular iterate. The term metaheuristic refers to methods that combine information about the cost with some heuristics in order to determine which candidate solutions to keep and how they should evolve. This combined measure of the candidate solution's quality is referred to as *fitness function* [74]. Heuristics tend to be much more effective than performing a completely random search [74]. Different metaheuristic algorithms use different types of heuristics and/or fitness functions. We describe a few of the most popular metaheuristics in the battery parameter identification literature below.

Particle Swarm optimization (PSO) emulates the movement of swarms, such as a flock of birds or a school of fish [100]. The candidate solutions are referred to as particles, and their positions in parameter space are updated each iteration based on randomness as well as information about its own best position and the swarms best position. A better position is simply one with a lower value of the objective function. Fan [81] used PSO in two steps to identify 26 battery parameters. Rahman et al. [89] implemented PSO for identification of four ROM battery parameters and could show convergence for all parameters when fitted to charge and discharge data. The convergence of the method was however dependent on the selection of initial values. The basic PSO algorithm is known to have a number of issues, such as the inability to locate the optimal location even though the particles are swarming nearby. Shen and Li [94] applied a hybrid PSO-LM algorithm that uses PSO for the course scale and shifts to LM once convergence slows down near (a hopefully) global optima. This combines the global exploration of PSO with the fast convergence of LM. In their paper, they could show that the parameters of an empirical battery model estimated with the combined approach produced better voltage fit than parameters estimated with only PSO or only LM. This approach has to our knowledge not been explored for the DFN or SPM parameters.

Bacterial foraging optimization (BFOA) mimics the behavior of bacteria and includes four steps; chemotaxis, swarming, reproduction as well as elimination and dispersal. Similar to PSO, many potential solutions, here representing bacteria, are generated initially. Chemotaxis is the step when the bacteria move through space by taking steps in some direction. To also include the swarming behavior of bacteria, a fitness function is constructed that takes into account both the cost and the distance to other bacteria. If many bacteria are close together, it indicates an optimal region, and other bacteria will then be incentivized to move there. Ma et al. [86] identified six parameters of the SPM using BFOA. They used 40 bacteria and saw convergence after 80–100 chemotactic iterations.

Evolutionary algorithms are inspired by evolution in the sense that candidate solutions are treated as individuals in a population whose fitness to survive depends on their objective value. The Genetic algorithm (GA) is one of the most popular probabilistic global search algorithms. It is initialized with a set of random candidates. During each evolution process, new individuals are generated by fitness-proportionate selection, random crossover and mutation. It has been used by several authors for battery model PE [50,79,82,84,85,88]. The main benefit of GA is its ability to handle complex problems as well as the possibility of parallel implementation for faster computations [101]. Zhang et al. [50] implemented a parallelized GA to identify parameters of the DFN model and reported a speed up of 14 times compared to serial GA. Since a strategy for updating candidate solutions might not work equally good for the entire set of candidate solutions, Reddy et al. [91] combined three different evolutionary algorithms when optimizing 44 parameters of the DFN model. Each algorithm was run until convergence, and the next was initialized where the previous finished. They could show that switching between methods caused the cost function to keep decreasing where it would have otherwise plateaued.

Harmony search (HS) is a method in which the parameter vector is viewed as a harmony and each of the parameters symbolizes a pitch. New harmonies are generated using all of the previous harmonies. Chun et al. [51] used an adaptive exploration HS algorithm to identify 17 DFN model parameters. To more efficiently explore parameter space, they adjusted the search space adaptively based on each parameters

estimated variability. In comparison with other algorithms such as PSO and GA, their approach yielded faster convergence and higher accuracy (on synthetic data).

All methods discussed in this section involve a stochastic component. This allows them to escape poor local minima and saddle points and continue to make progress towards better solutions. However, the class of algorithms reviewed in this section tend to require a large number of iterations until they converge. It is therefore beneficial to narrow down the search space as much as possible [85]. We refer to [74] for more information on metaheuristic algorithms as well as other options for global optimization.

## 5. Parameter sensitivity

Parameter sensitivity is a measure of how a model's response is affected by its parameters [40]. It is an important concept for parameter identification since only sensitive parameters can be accurately identified. Conversely, if a sensitive parameter is given an inaccurate value, it will lead to larger model output error than if a non-sensitive parameter is wrongly parametrized. The sensitivity of a parameter is assessed using SA and depends on the model structure, the applied input and the method used to assess it. In addition, non-linear models can include parameter interactions such that the effect of one parameter depends on the values of other model parameters. SA can be used as a tool to choose which parameters to identify, investigate how parameter uncertainty affects the output uncertainty and to select data or design experiments that increase a parameter's sensitivity and thus its identifiability. Sensitivity analyses of physics-based battery models has been conducted with the purpose of increasing model understanding [102–104], assessing estimator performance [105], improving PE [57,84,93,106–108] and improving battery design [68,109]. An overview of sensitivity analyses of physics-based battery models are compiled in Table 4.

When performing a SA of the battery model, the target of interest can be any quantity that is studied by the model. However, few studies use SA for other targets than cell voltage. In the work of Li et al. [107], the parameter sensitivity was evaluated for the positive electrode surface SOC, positive electrode average SOC and negative electrode potential in addition to cell voltage. These battery states are relevant if the purpose of the model is to be used in a BMS. Their SA showed that the parameters that were insensitive to the cell voltage, and thus hard to identify from operational data, had little impact on the other battery states. Edouard et al. [106] added calendar aging to their simulation profile and studied parameters' impact on calendar aging. Lin et al. [68] studied how the cell capacity and maximum cell temperature are affected by the parametrization, in order to draw conclusions on how to improve battery cell design. SA is thus a tool not only for the parametrization process but also to gain understanding about how different battery properties affect each other.

The input signal that is used for the SA has a large effect on the outcome and should therefore be chosen in such a way that it corresponds to the model's intended usage. Samadi et al. [110] used random current pulses as input to their battery model and the result of their SA labeled the solid diffusion coefficients as hard to identify due to lack of sensitivity. Grandjean et al. [102] included a two hour rest period in their input signal and their SA resulted in the solid diffusion coefficients being the most sensitive parameters. Zeng et al. [104] analyzed the sensitives of the SPM parameters for different input signals and observed that constant current (CC) charging and discharging excited capacity related parameters like electrode thicknesses and porosity while a vehicle drive cycle excited kinetic parameters (reaction rate constants, particle radii). These results might seem intuitive to a reader with experience in battery modeling, but they give a clue about the possibility to alter the input signal in order to affect a parameter's sensitivity. It also illustrates why it might be inappropriate to select, for example, a CC input to parametrize a model that will be used to simulate dynamic load cycles. This is further developed in Section 7 about experiment design.

A qualitative comparison of results from SA of cell voltage to the DFN model parameters using CC charge and discharge experiments is given in Fig. 5. Parameter sets and SA method vary between the included references. No clear consensus on sensitive parameters could be found. Some parameters, such as the capacity related active material volume fractions $\epsilon_{\pm}$ and the electrode thicknesses $L_{\pm}$ are consistently sensitive. Other parameters' sensitivities, such as diffusion coefficients in active materials and electrolyte $D_{\pm}$, $D_e$ seem to depend on the choice of SA, the studied parameter set, the nominal parameter values as well as assumptions for parameters that are not included in SA. It should also be noted that most SA map the uncertainties of the parameters to uncertainty of the output. Thus, the assumption on parameter uncertainty, i.e. the ranges in which the parameter is assumed to lie and its probability distribution inside those ranges, is crucial for the result. The following sections describe commonly used SA methods, highlighting differences as well as potential advantages. Software implementations of sensitivity analysis methods exist e.g. in COMSOL, Matlab [111,112] and Python [113,114].

### 5.1. Methods used for SA

The various methods for SA are classified as either global or local [40]. Global SA takes into account the sensitivity of parameters varying in the whole physics-constrained parameter space whereas local SA only studies perturbations near some nominal values. Since the true value of a parameter is rarely known, the nominal value of parameter $\theta_j$ is assumed based on literature, system knowledge or PE [40]. If the model is nonlinear only global SA will provide a robust measure of sensitivities [115]. Global SA is however more computationally expensive to perform due to a higher number of required model simulations [115]. An alternative classification of methods is based on how the parameter vector is sampled. One-at-a-time (OAT) methods vary only one parameter before each model evaluation while in All-at-a-time methods, all parameters are varied simultaneously [116]. The latter allows for a better analysis of the effect of parameter interactions but requires more model evaluations to reliably estimate the sensitivity [116]. The following sections describe further some common methods, selected due to their use in SA for physics-based battery models. For information on other SA methods, the reader is referred to [116,117].

#### 5.1.1. Local sensitivity analysis

A simple and intuitive way of assessing the sensitivity, $s$, of the output $y(k,\boldsymbol{\theta})$ to a parameter $\theta_j$ is to compute its partial derivative

$$s_j(k) = \frac{\partial y(k,\boldsymbol{\theta})}{\partial \theta_j}\Big|_{\theta=\theta^*} \quad . \tag{26}$$

The expected impact on the output can be computed as $\Delta y(k,\boldsymbol{\theta}) = \Delta\theta_j s_j(k)$, where $\Delta\theta_j$ represents the parameter uncertainty [115]. However, this expression will be valid only for linear models. If the model is non-linear, the value of the derivative will change depending on the value of $\boldsymbol{\theta}^*$. Despite this flaw, derivative-based SA is frequently used for non-linear models because of its simplicity and cheap computation [116]. It is then a local method since it only reveals information about the sensitivity of a parameter in the vicinity of $\boldsymbol{\theta}^*$. Local sensitivity of the physics-based battery models have been studied using partial derivatives that were computed numerically with the central difference method [110] and automatic differentiation [118] or derived analytically [103]. Local SA with numerical derivation requires at least $N_\theta + 1$ model evaluations. If the model is described as a dynamical system (see Eqs. (1) and (2)) the time series of local parameter sensitivities can be obtained by evolution of the sensitivity dynamical system

$$\mathbf{S}_x(k+1) = \frac{\partial \mathbf{f}_d}{\partial \mathbf{x}}\mathbf{S}_x(k) + \frac{\partial \mathbf{f}_d}{\partial \mathbf{z}}\mathbf{S}_z(k) + \frac{\partial \mathbf{f}_d}{\partial \boldsymbol{\theta}} \tag{27a}$$

**Table 4**
Sensitivity analyses of physics-based battery model parameters.

| Author | Model | Domain | Method | Target of interest | Input |
|---|---|---|---|---|---|
| Edouard et al. 2016 [106] | SPMe + thermal + aging | Local | OAT | Cell voltage, skin temperature, remaining capacity | CC discharge. Calendar aging time |
| Gao et al. 2021 [57] | DFN | Global | Monte Carlo + partial correlation | Cell voltage RMSE | CC charge, EV drive cycle |
| Grandjean et al. 2019 [102] | SPMe | Global | Morris | Cell voltage | CC charge, CC discharge, rest |
| Jokar et al. 2016 [84] | SPMe | Local | Derivatives | Cell voltage | CC discharge |
| Lai et al. 2019 [103] | SPM | Local | Derivatives | Cell voltage | CC discharge, current pulsing |
| Bi and Choe, 2018 [78] | DFN | Local | OAT | Cell voltage RMSE | CCCV charge, CC discharge |
| Li et al. 2020 [107] | DFN | Local | OAT | Cell voltage, positive electrode bulk and surface SOC, negative electrode potential | CC charging, EV drive cycle |
| Lin et al. 2018 [68] | DFN + thermal | Global | Variance | Max temperature, discharge capacity | CC discharge |
| Liu et al. 2020 [109] | DFN + thermal | Local | OAT | Cell voltage, polarizations | CC discharge |
| Scharrer et al. 2013 [93] | DFN | Global | Morris | Cell voltage | EV drive cycle |
| Vasquez-Arenas et al. 2014 [105] | DFN + thermal | Local | OAT | Cell voltage | CC discharge |
| Zeng et al. 2019 [104] | SPM | Global | Morris | Cell voltage | CCCV charge, CC discharge, EV drive cycle |
| Zhang et al. 2014 [108] | DFN + thermal | Local | OAT | Cell voltage, shell temperature | CC discharge |

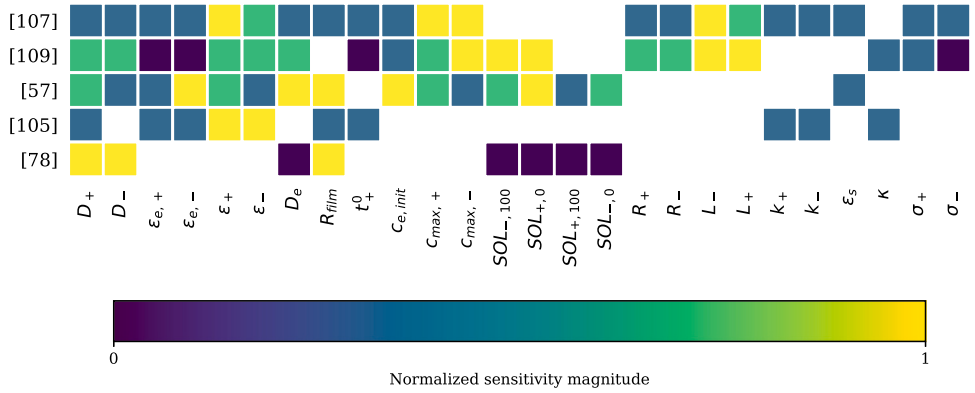


**Fig. 5.** Qualitative comparison of SA results in references [57,78,105,107,109] using the DFN model. Sensitivities are ranked from insensitive, to very sensitive in four discrete levels. All results are for CC discharge or charge experiments. Where numerical values were not published, data was extracted from result-figures. All five references investigate different parameter sets and employ different SA methods. Parameters only investigated in a single reference are omitted.

$$\mathbf{S}_z(k) = \frac{\partial \mathbf{g}}{\partial \mathbf{x}}\mathbf{S}_x(k) + \frac{\partial \mathbf{g}}{\partial \mathbf{z}}\mathbf{S}_z(k) + \frac{\partial \mathbf{g}}{\partial \boldsymbol{\theta}} \tag{27b}$$

$$\mathbf{s}(k) = \frac{\partial h}{\partial \mathbf{x}}\mathbf{S}_x(k) + \frac{\partial h}{\partial \mathbf{z}}\mathbf{S}_z(k) + \frac{\partial h}{\partial \boldsymbol{\theta}} \tag{27c}$$

where $\mathbf{s}(k) = \partial y(k,\boldsymbol{\theta})/\partial \boldsymbol{\theta}$, $\mathbf{S}_x(k) = \partial \mathbf{x}(k,\boldsymbol{\theta})/\partial \boldsymbol{\theta}$ and $\mathbf{S}_z(k) = \partial \mathbf{z}(k,\boldsymbol{\theta})/\partial \boldsymbol{\theta}$ [118].

In addition to the derivative-based sensitivity measure described above, SA can also be variance-based. A variance-based OAT method has been used for parameter SA of the SPM [106] and the DFN model [78,105,107–109]. In the common approach, a reasonable range for each parameter is defined and $n$ values in that range selected (based on some assumed distribution, often uniform). The sensitivity of output $y(k,\boldsymbol{\theta})$ to a parameter $\theta_j$ is evaluated as the standard deviation of the output when varying the parameter within its range and keeping the other parameters constant:

$$s_j(k) = \sqrt{\frac{1}{n}\sum_{i=1}^{n}\left[y(k,\theta_j^{(i)}) - \frac{1}{n}\sum_{i=1}^{n} y(k,\theta_j^{(i)})\right]^2} \quad . \tag{28}$$

Most papers used $n = 10$. This method can still be considered local since it does not investigate the full parameter space but performs explorations in one dimension at a time, from a baseline point in the parameter space [119]. The higher the dimension of parameter space, the smaller the portion that is explored by this method (see [120] for a simple graphical proof of this). However, averaging the effect of several parameter realizations is sometimes termed robust local sensitivity because it covers a larger part of parameter space compared to using only partial derivatives [41]. Because the parameters are not varied simultaneously, this method cannot take into account interactions between parameters.

### 5.1.2. Global sensitivity analysis

Morris method, also known as the Elementary Effect Test is a global OAT method based on averaging several local differentiation measures, scattered over parameter space. It is a popular screening method for global SA, since it requires relatively few model evaluations, and it has been used to study the SPM [102,104] and DFN model [93]. However, the method only provides insight in which parameters are more important or less important, but cannot be used to quantitatively assign relative importance [40]. It is therefore suitable for tasks like ranking parameters based on their sensitivities or selecting sub-sets of non-important parameters or parameters that are hard to identify [121].

The procedure of Morris method is as follows. First, a set of parameters $\boldsymbol{\theta}^{(i)} = (\theta_1^{(i)}, \ldots \theta_{N_\theta}^{(i)})$ is sampled from some assumed distribution. This represents a point in parameter space. Second, one parameter is perturbed while the rest remain the same, and the model output is computed. Keeping the previously changed parameter value, another parameter is then changed and the model evaluated. This is done until all parameters have changed their values. It has produced a trajectory in parameter space. The elementary effect, $EE$, of the $i$th trajectory and

$j$th parameter is computed [104]:

$$EE_j^{(i)}(k) = \frac{y(k,\theta_1^{(i)},\dots,\theta_{j-1}^{(i)},\theta_j^{(i)}+\Delta_j^{(i)},\dots,\theta_{N_\theta}^{(i)}) - y(k,\theta_1^{(i)},\dots,\theta_{N_\theta}^{(i)})}{\Delta_j^{(i)}} \quad . \tag{29}$$

This is repeated for $n$ trajectories, and the mean and standard deviation of the $EE$ related to each parameter are used as sensitivity measures. A high mean signifies that the parameter has a large effect on the output, seen over the entire parameter space, while high standard deviation indicates that the effect of the parameter is non-linear or that it interacts with other parameters [40]. Note that the absolute value of each $EE$ can be used to avoid positive and negative values from canceling each other out [40]. The number of model evaluations for $N_\theta$ parameters is $n(N_\theta+1)$ where $n$ is the number of trajectories, often between four and ten [117]. For the same number of model evaluations, Morris method can better capture the true distribution of output values compared to local OAT [120].

It is clear that the sample size and sampling step greatly affect the result. A large sample step, $\Delta_j$, will increase the variation in parameter space but yield non-representative sensitivity measures if the model output's dependence on parameter $\theta_j$ is highly non-smooth [116]. Also the sampling method impacts the result. Random sampling is known to form clusters and therefore cannot guarantee good coverage of parameter space [122]. Zeng et al. [104] used Latin hypercube sampling to generate parameter sets for their analysis of the SPM model. It is a method that remembers previous samples and makes sure that there is only one sample taken from each hyperplane (corresponding to row and column in a 2-dimensional cube). A sequence with points that are well spread out in space is referred to as having *low-discrepancy* [122]. Other alternatives are discussed further in [116,122] and references therein.

Variance-based SA, also called Sobol's method, is standard in global SA [40,123]. Its main principle is that the total variance of model output, $V[y(k,\theta)]$, can be decomposed into parameter variances, $V_j(k)$, and variances associated with parameter interactions according to [124]

$$V[y(k,\theta)] = \sum_{j=1}^{N_\theta} V_j(k) + \sum_{j=1}^{N_\theta}\sum_{j<m}^{N_\theta} V_{j,m}(k) + \cdots + V_{1,2,\dots,N_\theta}(k) \quad . \tag{30}$$

It includes parameter interactions between all combinations of two parameters, $V_{j,m}(k)$, up until interaction between all $N_\theta$ parameters. Sobol's sensitivity index of the first-order effect of the $j_{\text{th}}$ parameter is defined as [124]

$$S_j(k) = \frac{V_j(k)}{V[y(k,\theta)]} \quad . \tag{31}$$

The statistic for performing the analysis is usually created using Monte Carlo simulations and the partial variance due to the first-order effect can be estimated from [40]

$$V_j(k) = V_{\theta_j}[E_{\theta_{\sim j}}[y(k,\theta)|\theta_j]] \approx \frac{1}{n}\sum_{i=1}^{n} y(k,B^{(i)})\left(y(k,A_{B,j}^{(i)}) - y(k,A^{(i)})\right) \quad , \tag{32}$$

where $E_{\theta_{\sim j}}[y(k,\theta)|\theta_j]$ is the expectation of the output when varying all parameters but $\theta_j$. The $n\times N_\theta$ matrices $A$ and $B$ each contain $n$ samples of $N_\theta$ parameters. In the matrix $A_{B,j}^{(i)}$, the $j$th column of $A$ has been replaced by the $jth$ column of $B$. The superscript $(i)$ denotes the sample, i.e. the row of the matrices.

The total effect of parameter $j$ on the output is evaluated as [125]

$$S_{Tj}(k) = \frac{V_j(k) + \sum_{m\neq j} V_{j,m}(k) + \cdots + V_{1,2,\dots,N_\theta}(k)}{V[y(k,\theta)]} \quad , \tag{33}$$

with Monte Carlo approximation [40]

$$V_j(k) + \sum_{m\neq j} V_{j,m}(k) + \cdots + V_{1,2,\dots,N_\theta}(k) = E_{\theta_{\sim j}}[V_{\theta_j}[y(k,\theta)|\theta_{\sim j}]] \approx \frac{1}{2n}\sum_{i=1}^{n}\left(y(k,A^{(i)}) - y(k,A_{B,j}^{(i)})\right)^2 . \tag{34}$$

The discussion on parameter sampling is valid also here; the sampling method affects how well spread out in parameter space the samples turn out. If a low-discrepancy sequence is used instead of a random sequence, the method becomes quasi-Monte Carlo [122]. Variance-based SA is a challenge in battery modeling due to the expensive model evaluation; the Monte Carlo method in Eqs. (32) and (34) requires $(2+N_\theta)n$ model executions where $n$ is typically 500–1000 [117].

Some alternative approximations of the variance contributions have been proposed, such as Fourier series expansion methods or emulator methods [116]. Lin et al. [68] performed global SA of a 3D multi-physics battery model using the principles of Sobol's method and employing polynomial chaos expansion. With polynomial chaos expansion, the model response was approximated by a linear combination of orthogonal polynomial basis functions, and the associated coefficients were used to compute the expectations and variances needed for the Sobol indices. This reduced the number of required model evaluations. Sudret [126] showed that high-order polynomial chaos expansion based evaluation of Sobol indices is in fact analytical.

Another method to compute first order contributions to model output was employed by Gao et al. [57]. In their paper, they used Monte Carlo simulations to generate parameter samples and corresponding voltage outputs. A cost function was defined as the root-mean-square of the error between simulated and experimentally measured voltage. The sensitivity of a parameter was subsequently computed from the correlation between the parameter in question and the cost function after removal of effects from all other parameters. This is referred to as partial correlation. They performed a convergence analysis that formed the basis for their decision to use 900 samples per parameter to obtain their statistics.

## 6. Parameter identifiability

In Section 5, we established the requirement of parameter sensitivity for identifiability. In this section, the concept of identifiability is examined deeper. A parameter is considered identifiable if it is theoretically possible to determine a unique optimal value from measurements [127]. Unidentifiability of a parameter can have three sources; model structure, parameter variance (from noise and model errors) as well as lacking excitation of model dynamics with the input signal [95]. The first source only concerns the structure of the model equations. Consider a trivial example; the parameters of a model

$$y(t,\theta) = (\theta_1+\theta_2)u(t) \tag{35}$$

can only be identified as a sum and never separately. The latter two sources are of practical nature since they consider the impact from the experimental data. The concept of practical identifiability is closely related to parameter sensitivity, as an increase in sensitivity also increases the identifiability. However, for a parameter to be identifiable it is not sufficient to have high sensitivity but it must also be possible to distinguish its effect on the output from other parameter's impact [95]. While varying sub-classifications of identifiability have been used in literature, Goshtasbi et al. [127] chose to differentiate only between structural and practical identifiability, which is the distinction used in the following sections as well.

The IA is often performed locally, with the parameter set that was found in the optimization procedure and with the purpose of verifying its (local) uniqueness [128]. This is because good model performance does not guarantee correctly identified parameters. It only implies that the parametrization performs well for the conditions and dynamics present in the chosen validation data. Unidentifiable

parameters are likely identified inaccurately and might be detrimental to model performance if an input for which they are sensitive is applied. IA can therefore be used to verify model validity, as a complement to testing the model on several distinct data sets. It should however be noted that a model can fail to replicate new data due to other reasons than identifiability issues, such as structural errors (introduced in Section 2) [32]. IA can also be conducted before PE, to select a subset of parameters to identify (see e.g. Jin et al. [83]). Also in this case, the results are often based on a local study around some assumed nominal parameter values.

### 6.1. Structural identifiability

Structural identifiability analysis [129] investigates the model structure without considering input or output data. Ljung and Glad [130] defined a global identifiability criterion for a model $K(t,\theta)$. Considering

$$K(t,\theta) = K(t,\theta^*) \quad , \tag{36}$$

a model is

- globally identifiable if Eq. (36) has one solution,
- locally identifiable if Eq. (36) has a finite number of solutions and
- unidentifiable if Eq. (36) has an infinite number of solutions.

Bizeray et al. [39] studied structural identifiability of a SPM. As the kinetics in SPM and DFN are non-linear, they first linearized the kinetic sub-model for small perturbations around a certain SOC. They found that the linearized SPM is structurally identifiable in the general case but note that zero half-cell potential gradient leads to structural unidentifiability. This implies that e.g. for a graphite Lithium–Iron–Phosphate (LFP) SPM, parameters are only structurally identifiable in very small SOC windows, as both half-cell OCV are largely flat. They left analysis of the non-linear model for future work. Drummond and Duncan [58] extended this work and studied a linearized DFN model. They similarly assumed small current perturbations. This allowed linearization of the Butler–Volmer equation Eq. (19) and implied that the battery states were approximately equal to their initial state. Additionally, state dependencies (such as SOC, $T$ etc., compare Table 2) in parameters was neglected. They showed that 21 model parameters characterize the model uniquely and concluded that a unique solution to the corresponding PE problem must then exist [58]. Note that the simplifying assumptions made in [39,58] hinder extrapolation of these results to the general SPM and DFN. A similar result is obtained by Khalik et al. [131]. They obtained a total of 24 identifiable parameters by reparameterizing the DFN model. This was achieved by normalizing model equations where e.g. Fick's law Eq. (22) was divided by the particle radii $R_{\pm}$ of the respective domains, yielding a diffusion time constant parameter. See Section 3.2 or reference [131] for a more in depth discussion. As they did not linearize the model or make other simplifications this result is generally valid for the investigated model.

### 6.2. Practical identifiability

Opposed to the structural identifiability which merely considers the make-up of a model, practical identifiability studies if the experimental data enables a unique solution of the parameter optimization problem. The existence of such a solution depends on the objective function $F$, and thus on the data, but not on the optimization algorithm [95]. The criteria for local practical identifiability can similarly to Eq. (36) be expressed as

$$F(\theta) = F(\theta^*) \tag{37}$$

having a unique solution $\theta = \theta^*$ in a neighborhood around $\theta^*$ [95]. Local identifiability thus means that $\theta^*$ is not necessarily the only parameter vector to produce a cost function value corresponding to $F(\theta^*)$ but that the cost function value changes for any perturbation of $\theta^*$ within the neighborhood. Considering the least-squares cost function, we obtain

$$F(\theta^*) = \sum_{k=1}^{N}\left(y(k) - \hat{y}(k,\theta^*)\right)^2 = \Delta\mathbf{y}^T\Delta\mathbf{y} \quad , \tag{38}$$

for the optimal parameter vector $\theta^*$. In the neighborhood of $\theta^*$, the model output $\hat{y}(k,\theta)$ can be approximated with a first-order Taylor expansion, as in the GN method. The least-squares objective function corresponding to $\theta$ is reformulated as

$$F(\theta) = \sum_{k=1}^{N}\left(y(k) - \hat{y}(k,\theta)\right)^2 \approx \sum_{k=1}^{N}\left(y(k) - \left(\hat{y}(k,\theta^*) + \frac{\partial\hat{y}(k,\theta)}{\partial\theta}\Big|_{\theta=\theta^*}(\theta-\theta^*)\right)\right)^2 = \Delta\mathbf{y}^T\Delta\mathbf{y} + 2[\mathbf{S}(\theta-\theta^*)]^T\Delta\mathbf{y} + [\mathbf{S}(\theta-\theta^*)]^T\mathbf{S}(\theta-\theta^*) \quad , \tag{39}$$

where $\mathbf{S}$ is the $N \times N_\theta$ *sensitivity matrix* with elements defined by

$$\mathbf{S}_{k,j} = \frac{\partial\hat{y}(k,\theta)}{\partial\theta_j}\Big|_{\theta=\theta^*} \quad . \tag{40}$$

Eq. (37) thus has a locally unique solution in $\theta = \theta^*$ only if the Hessian,

$$\mathbf{H} = \mathbf{S}^T\mathbf{S} \quad , \tag{41}$$

has linearly independent rows, i.e. full rank (since rank($\mathbf{S}$) =rank($\mathbf{S}^T\mathbf{S}$)). Gosthasbi et al. [127] provide a similar derivation. A column of the sensitivity matrix in Eq. (40) corresponds to the (local) sensitivities of parameter $\theta_j$ throughout the experiment. It is sometimes referred to as a sensitivity vector [127]. Another way of understanding local practical identifiability is that in order for $\theta_j$ to be identifiable, its impact on the output must be significant enough and unique enough [128]. The former connects to the relative magnitude of the sensitivity vectors whereas the latter relates to their linear independence [127]. Both criteria translate to attributes of the sensitivity matrix, such as its rank.

Motivated by the above derived criteria, practical IA involves studying different properties of the sensitivity matrix or the Hessian matrix. Identifiability in parameter identification has been widely investigated in literature from many domains. In battery literature, the issue is topic of several publications noted in Table 5. To give the reader a broader overview, references for a fuel-cell model [132] and a battery equivalent circuit model [133] are included. The criteria are described in the remainder of this section.

**Table 5**
Practical identifiability criteria in literature.

| Criterion | Reference |
|---|---|
| Hessian condition number threshold | [82],[128],[127] |
| Hessian eigenvalue threshold | [127] |
| Positive definite Fisher matrix | [133] |
| Fisher matrix eigenvalue threshold | [134] |
| Sensitivity matrix numerical rank | [37] |

López et al. [37] used singular value decomposition (SVD) to compute the number of well conditioned singular values of the sensitivity matrix, as a way to assess its numerical rank. They could then draw conclusions about the practical identifiability of a DFN model parametrization problem.

The eigenvectors of the Hessian in Eq. (41) constitute a set of orthogonal directions in parameter space and the corresponding eigenvalues are the second derivatives of the cost function Eq. (39) in those directions [95]. The eigenvalues of $\mathbf{H}$ thus equates to the curvature of the objective function in parameter space and as such, reveal whether a stationary point with zero gradient is a peak, or if it is either a saddle point or a flat surface [95]. A zero eigenvalue indicates that the cost function is flat in that direction, which means no unique solution exists. In practice, eigenvalues are rarely exactly zero but can

be very small. López et al. [135] noted that the presence of small eigenvalues in **H** is a discernible proof of identifiability issues. Note that an eigenvalue does not represent one parameter but could be associated with many or all. It is therefore not possible to compute the eigenvalues and draw conclusions about which parameters are identifiable. Goshtasbi et al. [127] investigated identifiability by comparing the smallest Hessian eigenvalue $\lambda_{min}$ to a threshold minimum eigenvalue $\lambda_{th}$ and declared a subset of parameters identifiable only if the corresponding Hessian eigenvalue was above said threshold. As the eigenvalues represent the cost function curvature, they control the convergence rate of gradient descent methods. Then, this definition of unidentifiability becomes "too expensive to identify" which is useful in a practical setting but not an absolute measure.

It should be noted that if all eigenvalues are small, the problem can be re-scaled. Therefore, it is more problematic if the eigenvalues have a large spread in magnitude. Goshtasbi et al. [127] analyzed the Hessian condition number

$$\kappa_H = \frac{\lambda_{max}(\mathbf{H})}{\lambda_{min}(\mathbf{H})} \quad , \tag{42}$$

with $\lambda_{max}$ and $\lambda_{min}$ denoting the largest and smallest eigenvalues respectively. This allows categorizing an identification problem as

- ill-conditioned if $\kappa_H$ is large
- well-conditioned if $\kappa_H$ is close to 1.

Forman et al. [128] studied the condition number as a function of included parameters and defined a threshold for what would constitute an identifiable parameter set.

Similar approaches use the Fisher information matrix [80,82,118,128] which is often expressed based on the sensitivity matrix **S** and the output error covariance matrix $\mathbf{Q}_y$:

$$\mathbf{I}_F = \mathbf{S}^T \mathbf{Q}_y^{-1} \mathbf{S} \quad . \tag{43}$$

The Fisher matrix can be seen as a measure of the information about a parameter that is contained in the data. A derivation can be found in [31, p. 217]. It can be noted from the derivation that the simplified expression of $\mathbf{I}_F$ in Eq. (43) only is valid under the assumption that the error is Gaussian with zero-mean and independent of the input. Deng et al. [80] selected the parameter subset that maximized the quotient of Fisher information matrix determinant and condition number. Adding further parameters to this subset reduced the Fisher matrix' information content and thus hindered identifiability. Liu et al. [133] defined local identifiability by a positive definite Fisher matrix, since all the eigenvalues of a positive definite matrix are strictly positive. Schmidt et al. [134] measured identifiability of parameters by defining a threshold Fisher-matrix eigenvalue. These eigenvalues estimate the lower boundary of variance contributions to the diagonalized Fisher matrix [134].

The methods described in this section are local in parameter space. Even if all parameters were to be deemed locally unique it is possible, and likely, that they are not the globally optimal parameter set. To ensure that a globally optimal unique solution exist, identifiability analysis must be conducted in combination with an exploration of parameter space. Global SA only reveals information about a parameter's average sensitivity throughout parameter space, but does not guarantee sensitivity or uniqueness at precisely the global optimum [95].

### 6.3. Parameter ranking and grouping

Ill-conditioning of the sensitivity matrix and the Hessian stems from low parameter sensitivities or parameter correlation. It is visible e.g. as a large spread in eigenvalues. This correlation can in principle be structural interdependence but more often stems from qualitative similarities e.g. solid diffusion time-constants in both negative and positive electrode. Structural interdependencies can be handled by model re-parametrization, as [131] have done. An ill-conditioned problem for a full set of $N_\theta$ parameters can be transformed into several well-conditioned problems for parameter subsets of size $m < N_\theta$. In practice, this means grouping the parameters based on their identifiability, and identifying one group of parameters at a time while keeping the others at some assumed constant values. Grouping, or subset selection, can be done using the identifiability measures discussed in the previous section. This can however be difficult in practice, since only studying matrix eigenvalues or condition numbers does not reveal which parameters cause identifiability issues.

Instead, there are other methods that can rank individual parameters. Several works [37,83,118,127] group battery parameters based on QR factorization, also referred to as Gram–Schmidt-orthogonalization, of the sensitivity matrix. It takes parameter correlation under consideration by evaluating how close to orthogonal the columns of the sensitivity matrix **S** are, yielding a parameter ranking where dependent parameters are ranked lowest and independent parameters highest. For a practical tutorial see e.g. [136]. A similar orthogonal ranking method was explored for a subset of DFN parameters by Samadi et al. [110]. Additionally, they presented a correlation method that assesses parameter dependencies with sample correlation of the sensitivity matrix columns.

Variance based methods rank the identifiability of a parameter based on its variance contribution [127,134]. Parameter variances can be estimated from the Fisher matrix or from Monte Carlo simulations, see for example [37]. In the SVD method, singular values of the sensitivity matrix are identified and parameters are subsequently ranked based on their dependence on ill-conditioned singular values [37]. We refer readers that are interested in more in-depth discussion and comparison of these methods to the work of López et al. [37,135]. In [37] they investigated a subset of eight DFN model parameters and found that variance-based ranking yielded one identifiable parameter, SVD yielded zero identifiable parameters and QR decomposition yielded three. The results are based on empirically defined identifiability thresholds as well as assumed nominal values.

## 7. Model based experiment design

Previous sections outline methods for optimization to estimate parameters from measured data and tools for their SA and IA. All of these methods can be used on any singular experiment, but in fact this analysis can be used to chose particular experiments with beneficial properties for PE. Most authors study the sensitivity to CC charging or discharging [68,78,84,102–109] or drive-cycles [93,104,107], as these are commonly accessible in BMS and easy to perform. Rajabloo et al. [90] illustrated how parameters are more or less sensitive at a certain SOC. They showed for various different chemistries that sensitivities to specific parameters depend on the SOC and also the C-rate, i.e., the current normalized by the nominal capacity. Zhang et al. [108] determined best conditions for identification by studying how parameter sensitivities with respect to cell voltage and surface temperature relate to different C-rates and temperatures. In Fig. 6 Rajabloo et al.'s result [90] for a LFP/Graphite cell is reproduced to highlight how certain battery states, like the SOC or the applied current influence sensitivity for model parameters. The diffusion coefficient in the positive electrode is sensitive at high SOC and low rate, while the initial concentration in the positive electrode particles and the positive electrode porosity are sensitive at high SOC but not influenced by the rate. This result and similar investigations by Edouard et al. [106] highlight that optimal conditions for PE exist. Unless structural unidentifiability can be shown, there must be at least one experiment for each parameter for which it is identifiable. However these conditions must not necessarily lie within normal operating conditions, or be at all physical. Only identifiable parameters can be determined accurately. Consequently, parametrizations will be error prone for conditions outside those used for PE if experiment design is not carefully considered.

The visualization of the SA from [90] in Fig. 6 shows that an applied low rate current at high SOC provides good data for PE of the positive

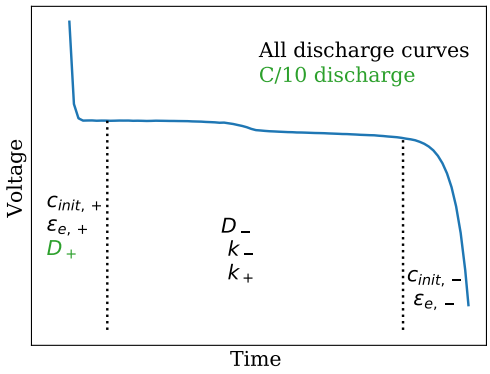


**Fig. 6.** Specific regions of sensitivity for certain parameters of a DFN model for a LFP/Graphite cell during CC discharging; reproduced from Rajabloo et al. [90]. They investigate positive and negative electrode porosity ($\varepsilon_{e,\pm}$), initial half-cell SOC (which is equated here with initial concentrations $c_{init,\pm}$), rate constant ($k_\pm$), and diffusion coefficient ($D_\pm$) for CC discharge curves up to 10 C. They find that for this case $D_+$ is only sensitive at a C/10 discharge while other parameter sensitivities are not rate dependent.

electrode diffusion coefficient $D_+$. In a more methodological manner, one can derive a measure of information contained in any certain experiment and algorithmically find an experiment that maximizes any such measure. This methodology is known as Optimal Experiment Design (OED). In this section we will discuss literature that uses OED to improve PE in physics-based Li-ion battery models.

### 7.1. Local optimal experiment design

Local OED (LOED) uses many of the techniques introduced in Sections 5 and 6. The Fisher information matrix $\mathbf{I}_F$, defined in Eq. (43), can be interpreted as a measure of the total information content about a set of unknown parameters for a given experiment. The inverse of $\mathbf{I}_F$ is a lower bound of the covariance matrix of an unbiased estimator. This is named the *Cramér–Rao bound* [31]. Maximizing Fisher information can thus decrease the parameter covariance and thereby yield tighter confidence bounds and increased parameter identifiability. Consequently, a strategy to design experiments aims to maximize Fisher information. Park et al. [118] noted that the three most used criteria in OED are:

- D-optimality: minimize $\log\det(\mathbf{I}_F^{-1})$
- A-optimality: minimize $\text{trace}(\mathbf{I}_F^{-1})$
- E-optimality: minimize $\lambda_{max}(\mathbf{I}_F^{-1})$

Schenkendorf et al. [41] also cited the E* criterion

- E*-optimality: minimize $\frac{\lambda_{max}(\mathbf{I}_F^{-1})}{\lambda_{min}(\mathbf{I}_F^{-1})}$

The problem can be interpreted geometrically to give an intuitive understanding of the different designs. The Fisher information matrix represents a joint confidence region of all parameters. D-optimality maximizes its determinant, or minimizes that of its inverse. This corresponds to minimizing the volume of the confidence region. Similar interpretation of remaining designs are e.g. discussed in [42]. Park et al. [118] and Forman et al. [137] used a D-optimal design in their study of the DFN model, while Pozzi et al. [138] used an A-optimal design for their SPM LOED. Schenkendorf et al. [41] showed how the choice of criterion can impact the resulting experiment. For instance, the most used D-optimal design overemphasizes the importance of the most sensitive parameter [42], whereas the A-criterion is unreliable for models with significant parameter interdependence [42]. E-optimal design has to the authors knowledge not been used for OED in physics-based battery models.

To highlight the benefit of an OED approach, Park et al. [118] compared the parametrization of a battery through OED with a conventional approach, for which they used a series of seven CC charge and discharge curves as well as a drive cycle. They showed that their approach reduced the RMSE from 36.1 mV to 25.5 mV for 1C discharge from 100 to 10% SOC. Neither Pozzi et al. [138] nor Forman et al. [137] validated their methods with real data.

**Table 6**
Design measures for GOED, reproduced from [41], $\overline{S}_j$ is the time averaged Sobol index for parameter $j$. The objectives are stated as minimization problems.

| Name | Cost function |
|---|---|
| 1. Shannon entropy (entire time horizon) | $1/\left(\sum_{j=1}^{N_\theta} \overline{S}_j \ln(\overline{S}_j)\right)$ |
| 2. Shannon entropy (at time $t = k$) | $\sum_{k=1}^{N}\sum_{j=1}^{N_\theta} S_j(k)\ln(S_j(k))$ |
| 3. Parameter dependency | $\sum_{k=1}^{N}\left(1-\sum_{j=1}^{N_\theta} S_j(k)\right)$ |
| 4. Overall output uncertainty | $1/\left(\sum_{k=1}^{N}\sigma^2(y(k,\theta))\right)$ |

### 7.2. Global experiment design

Generally the OED method is independent of the source of the sensitivity metrics. This means the LOED criteria can be used for global OED (GOED), with $\mathbf{I}_F$ simply being constructed from Sobol indices as opposed to local sensitivity indices. There are however several advantages of global sensitivity indices that enable the definition of alternative designs. Schenkendorf et al. [41] propose the criteria in Table 6. Criterion 1. balances all Sobol indices (Eq. (31)) to make all parameters sensitive throughout the experiment. Criterion 2. penalizes more than one parameter being sensitive at the same time. Criterion 3. reduces parameter interaction, as the sum of all first order indices at each time approaches one for zero parameter dependency. Finally, criterion four aims to maximize the total observable variance. All these criteria are then combined into a multi-objective optimization problem. While the solution can only be pareto-optimal, the inclusion of an objective that minimizes interaction makes this method especially attractive for cases with parameter interdependence. The largest advantage however stems from the global information provided by global SA and the fact that a global SA is independent of the initial guess for the parameter vector $\theta$. Pozzi et al. [139] show the benefits of GOED by comparing it with LOED using a SPMe model and synthetic data, i.e. data generated by the same model. In their case study they define a GOED efficiency metric $\eta = \frac{V_l oc[\theta_j]}{V_g[\theta_j]}$ to compare a parameter $\theta_j$'s variance using a local ($V_l oc[\theta_j]$) and global ($V_g[\theta_j]$) D-optimal design. They construct the Fisher information matrix $\mathbf{I}_F$ (Eq. (43)) based on local sensitivity indices for the local D-optimal design and on Sobol indices for global D-optimal design respectively. Even when using the same initial conditions and constraints for both local and global design they show that a global approach increases the model output variance by factors ranging from 1.005 to 17.65 indicating better identifiability.

### 7.3. Experiment definition

An important aspect of OED is the definition of the experiments that shall be optimized. Park et al. [118] used a pre-defined library of input experiments based on sinusoids, pulses and driving cycles. They normalized the experiments so all of them have similar charge throughputs. Lengths were allowed to vary between 600 and 3600 s and a maximum C-rate of 5C was set. Tests were run at 20, 40, 60 or 80% SOC. Finally they investigated a total number of 738 experiments and selected the optimal ones of the set. Pozzi et al. [138] divided their experiments in sub-sections of constant input currents and performed OED for each of these CC sections. When all sections were evaluated, the optimal experiment was a concatenation of all sub-sections. They started all the experiments at 100% SOC. Forman et al. [137] optimized every data point in a 600 s experiment with 5 Hz sampling. In essence, all three papers presented here designed their inputs based on a combination of initial conditions, experiment duration, experiment dynamics

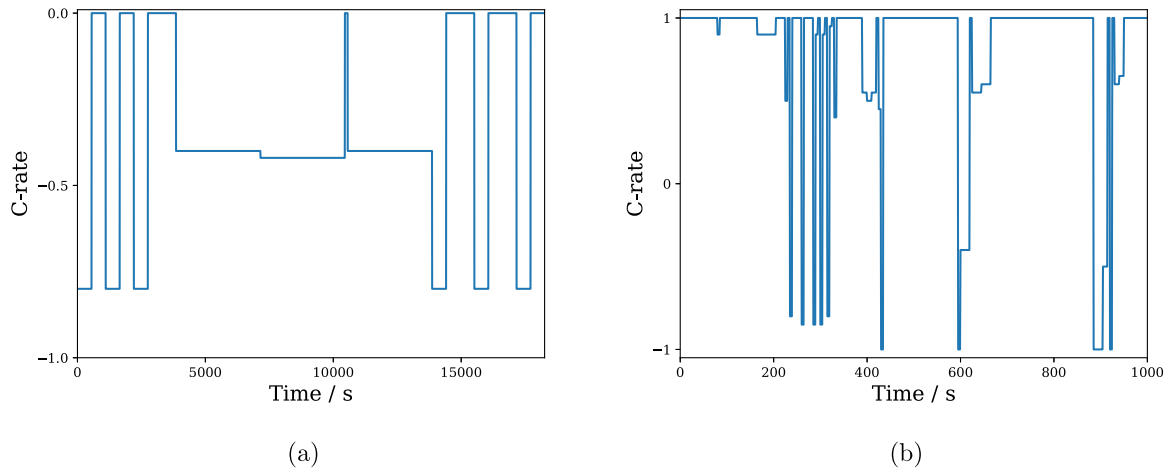


**Fig. 7.** Adapted derived optimal experiments by (a) Park et al. [118] (with permission, Copyright 2018 IOP publishing) and (b) Pozzi et al. [138] (with permission, Copyright 2018 American Chemical Society). (a) is optimal for a parameter sub-group including particle radii in positive and negative electrode, while (b) is the first of a set of ten consecutively performed optimal experiments derived for their set of seven parameters, including the Bruggeman coefficient, the cathodic transference number, diffusion coefficients for electrolyte and both electrodes and finally kinetic rate constants for both electrodes.

and experiment shape. A comparison of resulting experiments is shown in Fig. 7. It is clear that experiments can only be optimal within the allowed space of possible experiments. A challenge that remains is thus the algorithmic generation of experiments that covers a wide range of different experiments with only few design parameters. A wider experiment space can however result in optimal experiments that are very different from a models intended use. This can be problematic in the case of significant structural model errors [32], as parameters will be identifiable but structural errors may dominate when attempting model extrapolation.

## 8. Machine learning for parameter identification

ML encompasses techniques for automated learning of patterns in data. A ML model is a typical example of a black-box model, where functions map the input data to the output data without involving any known physical relations. Neural networks (NN) [140], support vector machines [141] and Bayesian networks [142] are examples of ML models with applications in a wide variety of fields. In recent years, procedures involving ML techniques has been proposed as alternatives to conventional battery model PE [2,143,144]. The workflow of such an approach, Fig. 8, is as follows. First, a large amount of data is generated by simulating the output of a physics-based battery model for different input signals and different parameter sets. Second, a ML model is trained to learn the parametrization of the battery model from the dynamics of the input and output. Third, the ML model can be fed with measured battery signals and provide an estimate of the underlying parameters. The benefit of this kind of method is that once the model training is completed, low computational effort is required to obtain model parameters from data. This implies that the ML model could be implemented to provide updated information about aging sensitive parameters while the battery is in use. It could also be an efficient tool for end-of-line characterization for battery manufacturing [2].

To parametrize a battery model, Chun et al. [143] employed a long short-term memory model which is a type of NN. A NN comprises layers of artificial neurons that, like neurons in a human brain, transmit and receive signals. The first layer takes the input data, which is then propagated through the network from one layer of neurons to another. The output of each neuron is a non-linear function of the sum of its weighted inputs [140]. Training a NN means optimizing the weights such that the output of the final layer best fits the training data. In their paper, Chun et al. [143] chose to identify six parameters of the DFN model that are likely to change during the battery's course of aging; the solid particle surface areas, the solid particle conductivities as well as the solid electrolyte interphase layer thickness and remaining total capacity. A total of 168,000 data sets was generated for training and validation, each of which was 100 s long and produced from varying parameter values according to assumed aging trajectories. They validated their estimation on synthetic and measured data, the latter yielding voltage errors of less than 18–26 mV. Jokar et al. [144] trained a NN to identify five parameters of the SPM from a 1C discharge curve. Turetskyy et al. [2] used NN to train a surrogate for the DFN battery model to return a set of seven model parameters for given cell voltage measurements. Kim et al. [142] estimated six DFN model parameters using deep Bayesian Harmony search. They used a deep Bayesian NN to learn the dynamics of the DFN model and output a parameter probability distribution given input signals. This distribution was used to guide the search space in the HS optimization algorithm. They compared their method to conventional optimization schemes such as LM, PSO and GA, and could show that their method required fewer model evaluations as well as lower PE error than the other algorithms.

An important note is that the predictive ability of ML models are fully dependent on the data that was used to train it. If it is subjected to input that was not part of the training range, there is no guarantee the model will output something even physically possible. This points to the challenge of designing the training data in a way that represents all the real scenarios, without having to analyze a, for the application, impossible amount of combinations between different parameter values.

There exist a multitude of software tools for building machine learning models. Some examples include Tensorflow [145], PyTorch [146], Scikit-learn [147] and Matlab's Statistics and Machine Learning Toolbox. Detailed descriptions of ML approaches is outside the scope of this review paper. The interested reader is referred to e.g [140,141,148], in addition to the other citations in this section, for more information. For a perspective on how physics-based battery models can be used in conjunction with ML models, see [149].

## 9. Validation

Any modeling or parametrization study shall include some kind of validation step. In most cases, this is done by looking at the quality of the model output prediction. Less frequent but nevertheless relevant is the direct assessment of parameter estimates. Their performance can be evaluated either statistically or by comparison to experimental measurements.

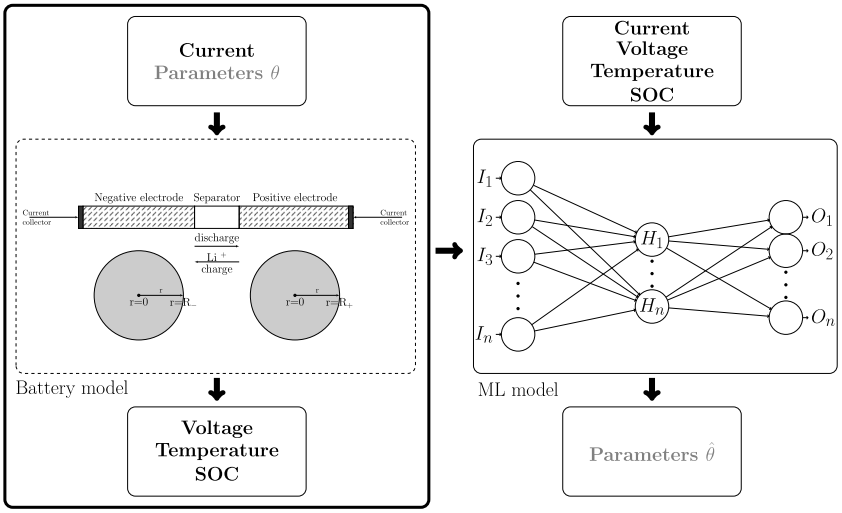


**Fig. 8.** Approach for using ML to estimate battery model parameters.

### 9.1. Experimental validation

Electrochemical methods are used to measure the battery response to cell voltage or current. They are commonly complemented by analytical methods such as scanning-electron-microscopy (SEM) or x-ray photoelectron spectroscopy (XPS) [150]. Electrochemical methods are most often employed to characterize commercial cells directly or on laboratory cells build from harvested or synthesized material. Such data might e.g. be available in BMS or lab-scale cycling studies. In this configuration it is difficult to separate properties of positive and negative electrode. In lab-scale cells a lithium metal is therefore often used as reference and counter electrode together with either positive or negative working electrode. These half-cells can reduce the number of unknowns assuming that the lithium counter electrode is not rate determining. However, the influence of lithium counter electrode and its parameters cannot always be totally ruled out. Therefore, a reliable approach is the measurement in three-electrode-cells, where, additionally to working and counter electrodes, a reference electrode is employed. This allows the separation of working and counter electrode signals while still in full-cell configuration. Typical physical and electrochemical techniques used in conventional parametrization are *post mortem*. Waldmann et al. [151] give an elaborate review on post-mortem characterization techniques.

SEM is common in determining particle size or particle size distribution and Hg porosimetry or Brunauer–Emmett–Teller (BET) measurements in determining the electrode porosity and surface area. The lithium diffusion coefficient in the active material is an often sought after parameter, but only rarely obtained by physical characterization such as nuclear magnetic resonance (NMR) [152] and neutron or muon microscopy [153]. 3D visualization techniques like X-ray tomography microscopy and focused-ion beam SEM (FIB-SEM) allow the quantification of microstructural properties, e.g. porosity, tortuosity, specific surface area and particle size [65,154]. Electrochemical methods like galvanostatic intermittent titration technique (GITT) [155], electrochemical impedance spectroscopy (EIS) [156], CC cycling, hybrid power pulse characterization and cyclic voltammetry are carried out to extract kinetic and transport properties of electrode active materials. The most common parameters determined this way are diffusion coefficient and kinetic rate constant or exchange current density. Together these constitute a conventional PE study.

For thorough parametrization studies using conventional methods we refer readers to [22–26]. Note that due to model assumptions and simplifications it is not guaranteed that the experimentally determined parameter set is optimal in terms of model performance. For this reason authors commonly perform a fitting procedure or manually tweak experimentally measured model parameters [22,24] to decrease model error.

### 9.2. Statistical validation

Unless synthetic data has been used or careful experimental characterization has been performed (compare Section 9.1), the true model parameters remain unknown. True parameters with physical interpretation might not even exist, if a model is a very simplified description of the real process. Discrepancy between model and reality also means that even when parameters are analytically measurable, those parameter values might not result in the best model fit. Validation can therefore be conducted by studying the predictive performance of the model and the statistical properties of the parameter estimates.

In battery modeling works focused on PE, a common form of validation is to compare the simulated and measured output for charge and discharge curves [83–86,88,89] and/or dynamic current pulses [50,83,85,86,91]. The error, or *residual*, is defined as

$$e(k,\hat{\boldsymbol{\theta}}) = y(k) - \hat{y}(k,\hat{\boldsymbol{\theta}}) \quad , \tag{44}$$

and apart from the magnitude of $e(k,\hat{\boldsymbol{\theta}})$, its correlation with other signals can also say something about how well the model captures the true system dynamics [31]. Forman et al. [82] computed the correlation between the residual and the input current and concluded that internal resistance was well captured by their model since no linear correlation could be seen. Since the battery dynamics is SOC dependent, they also evaluated correlation to SOC to see if this dependence was captured sufficiently well by the model. There will always be noise in the measured data so a perfect model that captures all real system dynamics should not have zero residual, but a residual that is just random noise [32].

The importance of cross-validation to ensure the model's validity outside of the training set was highlighted in Section 2. To ensure that the optimized parameters are applicable over a wide range of conditions, validation can be done on data with e.g. different temperatures and current rates [24,26].

IA can support or challenge the validity of the model. A parameter that is deemed unidentifiable, given its estimated value and the data that was used to produce it, is likely invalid. This is something that might not be discovered if only validation of model output is performed, especially if the validation data is similar or the same as the fitting data. López et al. [37] studied the estimator performance for a DFN model parameter identification problem. They concluded that

using a single discharge curve for identification lead to poor estimator performance for several parameters, despite the good fit between model output and training data. Such parameters can potentially cause large errors when other input signals are applied. If all parameters are identifiable, but the model still behaves poorly for data different than the training set, it could be a sign of structural errors, i.e. that the model structure cannot capture all of the processes in the real system well [32].

Because of structural errors and noise, all parameter estimates will be associated with some variability. The quality of the parameter estimates can thus be assessed in a statistical sense, without knowledge about the true parameters. The covariance matrix, $\mathbf{Q}_\theta$, of the parameter estimates can be obtained by performing parameter identification multiple times, on different data sets, to produce a distribution [32,37]. Since this is very time consuming, it is common to use the approximation [37]

$$\mathbf{Q}_\theta \approx \mathbf{I}_F^{-1} \approx [\mathbf{S}^T \mathbf{Q}_y^{-1} \mathbf{S}]^{-1} \quad , \tag{45}$$

even though it is an underestimate of the variance if structural errors and process noise is present (in nonlinear models) [32]. A large parameter variance is thus associated with large output variance (from noise) as well as low parameter sensitivity. The parameter variances can be used to set confidence bounds on the parameter estimates, as done in e.g. [37,82,92].

## 10. Summary and discussion

Parameter Estimation (PE) of physics-based battery models is a challenge facing engineers and researchers throughout the battery modeling community. The models typically include a large number of parameters, some of which cannot be measured explicitly. In addition, many applications require a parametrization strategy that is flexible and non-invasive. System identification is the process of fully or partially parametrizing a dynamical model from fitting of input–output measurement data. Fig. 1 summarizes the main steps of the process.

Normally, a modeling study begins with selecting or deriving a model that can represent the investigated system. Once a model is chosen, values must be assigned to its parameters. Many articles reviewed in Sections 5 and 6 have shown that, for their problem setup, only a subset of the parameters are sensitive and identifiable. This implies that the goal does not have to be to estimate all parameters from input–output data, as long as the modeler can determine which parameters are necessary and possible to identify in that way. As a first step in the parametrization procedure, a modeler should therefore determine which model parameters can accurately be measured , and which parameters must be assigned in other ways. A second step could be to analyze the structural identifiability of the model parameters. Structural identifiability analysis (IA) answers the question as to which model parameters are independent, and thus in theory possible to identify. Reviewed articles in Section 6.1 indicate that the battery models contain parameter interactions, such that some parameters cannot be identified from any data.

A parameter's importance can be quantified by its sensitivity; a sensitive parameter has higher impact on the resulting model output than an insensitive. Sensitivity analyses (SA) of battery model parameters are reviewed in Section 5. SA is used both before and after parameter optimization. Prior, it serves the purpose of selecting which parameters to optimize, and which to assume from literature or experience. It is also an important component in experiment design. After, it is a tool to assess identifiability and set parameter confidence bounds. A local SA is informative in the vicinity of given parameter values but can only say something general about a model's parameters and their importance if the model is linear. This implies that a global SA might be more suitable before parameter values are estimated, and that a local analysis can be employed afterwards, at the identified values. Many authors cited in Section 5 used local or one-at-a-time (OAT) SA around some nominal values despite the fact that physics-based battery models are non-linear with interactions between several parameters. Depending on the type of study, this might skew the results. Few SA have focused on the parameter sensitivity during real operation, in applications such as electric vehicles (EVs). This could be of relevance when developing electrochemistry-based battery management systems (BMS) as well as for *in-operando* parameter identification. Another observation is that most of the SA results, even the ones based on the same model and similar input signals, are very diverse. This shows that parameter sensitivities are dependent on the assumed parameter ranges and distributions, SA method used as well as all other values assigned to the model (e.g. geometry and stoichiometry). It is not advised to collect SA results from literature but to conduct a study specific for the model and application in question.

If a model is structurally identifiable there exists an experiment, albeit not necessarily a feasible one, for which each parameter's impact on the output can be detected. While some experiments are considered standard in the field there is no certainty they excite all model parameters. Model based optimal experiment design (OED, Section 7) can be used to find experiments maximizing e.g. Fisher information to excite desired parameters. Global sensitivity measures account for model non-linearities and parameter interaction and do not rely on accurate initial guesses for the parameter vector. Global OED is likely a better option in terms of accuracy, due to the characteristics of the battery models, whereas local OED does hold significant computational advantages. Reviewed literature shows that parametrization using OED can significantly improve model performance.

Once a subset of parameters is selected and experiments are performed, the parameters must be estimated by means of optimization. In Section 4 we review literature focusing on accurate and fast PE as well as exploration of novel optimization methods. No single method stands out as superior . Since the result of a local optimization procedure will depend on the initial guess, a global search might be beneficial if little is known about the parameters prior to the optimization. Combining a global and local search by method hybridization and homotopy transformation was successful in several works.

Practical IA, as outlined in Section 6, plays an important role in physics-based battery model parametrization as it reveals whether a unique solution to the identification problem exist. Intuitively, it measures whether a parameter's impact on the output is significant and unique enough for it to be separated from the other parameters. It can be used before PE to group parameters that likely can be identified simultaneously and after parameter optimization to verify the validity of the result. We highlight the strong connection of practical identifiability to sensitivity and note that practical IA inherits limitations of selected SA methods.

An alternative approach to parameter identification employs machine learning (ML), Section 8. Black-box models are then trained with vast sets of synthetic data, that is generated with a physics-based battery model. Once trained, these ML models can recognize underlying parameter values in experimental data, making them useful for in-operando PE. A drawback of ML models is their inability to extrapolate beyond training data.

We emphasize the importance of a thorough validation, Section 9, to ensure a parametrized model can generalize beyond the estimation data and meets the requirements that comes from its intended use in an application or as basis for a study. The purposes of performing parameter estimation differ; either the desired end-product is a model with good predictive abilities or a good estimate of the battery's internal parameters. In a hypothetical perfect model resolving every process in the battery accurately, this gap is zero. Validation can therefore include experimental validation by means of electrochemical and physical characterization techniques and statistical validation, in which model predictions are compared with experimental data. The former alternative is mainly used to validate that a parametrization

**Table 7**
List of abbreviations.

| Abbreviation | Full text |
|---|---|
| BET | Brunauer–Emmett–Teller |
| BMS | Battery management system |
| BFOA | Bacterial foraging optimization algorithm |
| CC | Constant current |
| CCCV | Consant current constant voltage |
| COBYLA | Constraint optimization by linear approximation |
| DFN | Doyle–Fuller–Newman model |
| EIS | Electrochemical impedance spectroscopy |
| EVs | Electric vehicles |
| GA | Genetic algorithm |
| GITT | Galvanostatic intermittent titration technique |
| GN | Gauss–Newton |
| GOED | Global optimal experiment design |
| HS | Harmony search |
| LM | Levenberg–Marquardt |
| LMR-NMC | Lithium–manganese rich - nickel–manganese–cobalt |
| LFP | Lithium iron phosphate |
| LOED | Local optimal experiment design |
| ML | Machine learning |
| NCA | Nickel-cobalt–aluminum |
| NM | Nelder–Mead |
| NN | Neural networks |
| MSE | Mean squared error |
| OAT | One-at-a-time |
| OED | Optimal experiment design |
| OCP | Open circuit potential |
| OCV | Open circuit voltage |
| P2D | Pseudo two dimensional |
| PDAEs | Partial differential algebraic equations |
| PE | Parameter estimation |
| PITT | Potentiostatic intermittent titration technique |
| PSO | Particle swarm optimization |
| RMSE | Root-mean-square-error |
| ROM | Reduced order model |
| SA | Sensitivity analysis |
| SEM | Scanning electron microscopy |
| SPM | Single particle model |
| SPMe | Single particle model with electrolyte |
| SOC | State-of-charge |
| SOH | State-of-health |
| SOL | State-of-lithiation |
| SVD | Singular value decomposition |

procedure yields physical parameters. However, since the model is a simplification of reality, the parameter that best fits the data might not correspond to a value obtained by other measurements, even when the model performs really well in terms of output predictions. This bias is discussed in Section 2 and in Section 9. In order to reasonably interpret the results of a parametrization study, it is important to be aware of the limitations of the model, as discussed in Section 3.4.

## 11. Conclusion

In recent years, many articles have been published in which parametrization of physics-based battery models from data is investigated. This review compiles this body of work as well as provides a more detailed introduction to the concepts used, including sensitivity, identifiability, optimization, optimal experiment design and model validation. Many of the reviewed methods facilitated the parameter estimation process and improved model performance. Several works showed that not all parameters are possible to identify from data, due to lack of sensitivity or independence. There is also consensus in literature that not all model parameters need to be accurately parametrized in order for the model to perform well. However, from comparing the different studies, we conclude that the important and identifiable parameter subsets differ significantly between studies because they depend on the input current, the assumptions on the studied parameters as well as on other model assumptions.

A common theme throughout the reviewed topics is the distinction between local and global methods. It is too rash to rule out local methods in general, as they can be highly useful in the model validation step. Their significant computational advantages and low complexity make them a convenient choice also for a priori analyses. The dependence on an initial estimate of the parameter vector can however mean that parameter optimization finds only a local minimum and SA drastically misrepresents sensitivity; an error which will then propagate into a subsequent OED study. In general, the bigger the region of possible parameter values, i.e. the parameter uncertainties, and the more nonlinear the model, the more global a method must be to avoid misleading results. We found that few reviewed articles included this discussion in relation to their method choice and subsequent interpretation of their results.

To conclude; in this paper we reviewed literature that investigates PE for Li-ion battery models, presented the established techniques, and highlighted areas of interest for further research. Concepts central to the PE process have been described and discussed in light of the specific challenges for battery modeling. At the same time, we note that the methods presented here are not limited to physics-based battery models, but applicable to models of all kinds.

## Abbreviations

See Table 7.

## Greek symbols, superscripts and subscripts

See Table 8.

## Nomenclature

See Table 9.

**Table 8**
List of greek symbols, superscripts and subscripts.

| Greek symbol | Meaning |
|---|---|
| $\theta$ | Parameter vector |
| $\beta$ | Bias |
| $\varepsilon$ | Volume fraction |
| $\tau$ | Tortuosity |
| $\sigma_{\pm}$ | Electronic conductivity |
| $\phi_{\pm}$ | Potential |
| $\eta_{\pm}$ | Overpotential |
| $\alpha_{a,c,\pm}$ | Anodic or cathodic charge transfer coefficient |
| $\alpha$ | Step size in derivative based optimization algorithms |
| $\kappa_H$ | Hessian condition number |
| $\lambda$ | Eigenvalue |
| $\lambda_{LM}$ | Levenberg–Marquardt step adjustment factor |
| **Superscript** | **Meaning** |
| $\hat{}$ | Estimate |
| eff | Effective |
| (i) | Iteration or sample number |
| **Subscript** | **Meaning** |
| LS | Least-squares |
| e | Electrolyte |
| ± | Positive or negative electrode |
| tot | Total |
| s | Separator |
| surf | Surface |
| loc | Local |
| g | Global |
| d | Discrete |
| max | Maximum |
| min | Minimum |
| $j$ | Parameter index |
| $m$ | Alternative parameter index unequal to j |
| init | Initial |
| y | Model output |
| $\theta$ | Model parameter input |

**Table 9**
List of nomenclature.

| Variables | Explanation |
|---|---|
| $x$ | Electrode depth variable |
| $r$ | Particle radius variable |
| $c$ | Concentration variable |
| $i$ | Current density variable |
| $t$ | Time variable |
| $k$ | Sampling instant variable |
| **Vectors and Matrices** | **Explanation** |
| $\boldsymbol{x}(t)$ | State variable vector |
| $\boldsymbol{z}(t)$ | Algebraic variable vector |
| $\boldsymbol{u}$ | Model input vector |
| $\boldsymbol{y}$ | Model output vector |
| $\boldsymbol{p}$ | Optimization step direction vector |
| $\boldsymbol{J}$ | Jacobian matrix |
| $\boldsymbol{I}$ | Identity matrix |
| $\boldsymbol{A}, \boldsymbol{B}$ | General matrices |
| $\boldsymbol{S}$ | Sensitivity matrix |
| $\boldsymbol{H}$ | Hessian matrix |
| $\boldsymbol{I_F}$ | Fisher information matrix |
| $\boldsymbol{Q}$ | Covariance matrix |
| **Battery constants and parameters** | **Explanation** |
| F | Faraday constant |
| R | Universal gas constant |
| $T$ | Temperature |
| $L_{\pm}$ | Electrode thickness |
| $t_{\pm}$ | Diffusion time constant |
| $t_{+}^{0}$ | Cationic transference number |
| $1+\frac{\partial f_{\pm}}{\partial \ln c_e}$ | Activity coefficient |
| $D_{\pm}$ | Diffusion coefficient |
| $R_{\pm}$ | Particle radius |
| $U_{\pm}$ | Electrode open circuit voltage |
| $a_{\pm}$ | Active material surface area |
| $k_{\pm}$ | Reaction rate constant |
| **Other nomenclature** | **Explanation** |
| $S$ | Sensitivity |
| $S_T$ | Total effect |
| $s$ | Local sensitivity |
| $N$ | Number of steps, outputs, parameters or states |
| $n$ | Number of samples |
| $F$ | Cost function |
| $E$ | Expectation |
| $V$ | Variance |
| $K$ | Model |
| $e$ | Error |

## CRediT authorship contribution statement

**Malin Andersson:** Conceptualization, Formal analysis, Investigation, Data curation, Writing – original draft, Writing – review & editing, Visualization. **Moritz Streb:** Conceptualization, Formal analysis, Investigation, Data curation, Writing – original draft, Writing – review & editing, Visualization. **Jing Ying Ko:** Formal analysis, Investigation, Data curation, Writing – original draft, Writing – review & editing, Visualization. **Verena Löfqvist Klass:** Writing – review & editing, Supervision, Funding acquisition. **Matilda Klett:** Writing – review & editing, Visualization, Supervision, Funding acquisition. **Henrik Ekström:** Writing – review & editing. **Mikael Johansson:** Writing – review & editing, Supervision, Funding acquisition. **Göran Lindbergh:** Writing – review & editing, Supervision, Funding acquisition.

## Declaration of competing interest

The authors declare that they have no known competing financial interests or personal relationships that could have appeared to influence the work reported in this paper.

## Acknowledgments

This work was funded by Swedish Electromobility Center and Swedish Energy Agency through the FFI program Energy and Environment (project number 47103-1) and Batterifondsprogrammet (project number 39059-1). It was conducted within the framework of Batteries Sweden BASE.

## References

[1] I.D. Campbell, K. Gopalakrishnan, M. Marinescu, M. Torchio, G.J. Offer, D. Raimondo, Optimising lithium-ion cell design for plug-in hybrid and battery electric vehicles, J. Energy Storage 22 (2019) 228–238, http://dx.doi.org/10.1016/j.est.2019.01.006.

[2] A. Turetskyy, V. Laue, R. Lamprecht, S. Thiede, U. Krewer, C. Herrmann, Artificial neural network enabled P2D model deployment for end-of-line battery cell characterization, in: 2019 IEEE 17th International Conference on Industrial Informatics (INDIN), IEEE, 2019, pp. 53–58, http://dx.doi.org/10.1109/INDIN41052.2019.8972181.

[3] J. Li, K. Adewuyi, N. Lotfi, R.G. Landers, J. Park, A single particle model with chemical/mechanical degradation physics for lithium ion battery state of health (SOH) estimation, Appl. Energy 212 (2018) 1178–1190, http://dx.doi.org/10.1016/j.apenergy.2018.01.011.

[4] J. Lee, O. Nam, B. Cho, Li-ion battery SOC estimation method based on the reduced order extended Kalman filtering, J. Power Sources 174 (1) (2007) 9–15, http://dx.doi.org/10.1016/j.jpowsour.2007.03.072.

[5] M.T. Lawder, P.W. Northrop, V.R. Subramanian, Model-based SEI layer growth and capacity fade analysis for EV and PHEV batteries and drive cycles, J. Electrochem. Soc. 161 (14) (2014) A2099, http://dx.doi.org/10.1149/2.1161412jes.

[6] X.-G. Yang, Y. Leng, G. Zhang, S. Ge, C.-Y. Wang, Modeling of lithium plating induced aging of lithium-ion batteries: Transition from linear to nonlinear aging, J. Power Sources 360 (2017) 28–40, http://dx.doi.org/10.1016/j.jpowsour.2017.05.110.

[7] S.J. Moura, J.L. Stein, H.K. Fathy, Battery-health conscious power management in plug-in hybrid electric vehicles via electrochemical modeling and stochastic control, IEEE Trans. Control Syst. Technol. 21 (3) (2013) 679–694, http://dx.doi.org/10.1109/TCST.2012.2189773.

[8] X. Hu, S. Li, H. Peng, A comparative study of equivalent circuit models for Li-ion batteries, J. Power Sources 198 (2012) 359–367, http://dx.doi.org/10.1016/j.jpowsour.2011.10.013.

[9] M.-K. Tran, A. DaCosta, A. Mevawalla, S. Panchal, M. Fowler, Comparative study of equivalent circuit models performance in four common lithium-ion batteries: LFP, NMC, LMO, NCA, Batteries 7 (3) (2021) 51, http://dx.doi.org/10.3390/batteries7030051.

[10] S. Han, Y. Tang, S.K. Rahimian, A numerically efficient method of solving the full-order pseudo-2-dimensional (P2D) li-ion cell model, J. Power Sources 490 (2021) 229571, http://dx.doi.org/10.1016/j.jpowsour.2021.229571.

[11] K.A. Smith, Electrochemical control of lithium-ion batteries [applications of control], IEEE Control Syst. Mag. 30 (2) (2010) 18–25, http://dx.doi.org/10.1109/MCS.2010.935882.

[12] N.A. Chaturvedi, R. Klein, J. Christensen, J. Ahmed, A. Kojic, Algorithms for advanced battery-management systems, IEEE Control Syst. Mag. 30 (3) (2010) 49–68, http://dx.doi.org/10.1109/MCS.2010.936293.

[13] A. Pozzi, M. Torchio, D.M. Raimondo, Film growth minimization in a Li-ion cell: a Pseudo Two Dimensional model-based optimal charging approach, in: 2018 European Control Conference (ECC), 2018, pp. 1753–1758, http://dx.doi.org/10.23919/ECC.2018.8550404.

[14] X. Lin, X. Hao, Z. Liu, W. Jia, Health conscious fast charging of Li-ion batteries via a single particle model with aging mechanisms, J. Power Sources 400 (2018) 305–316, http://dx.doi.org/10.1016/j.jpowsour.2018.08.030.

[15] E. Namor, F. Sossan, D. Torregrossa, R. Cherkaoui, M. Paolone, Battery storage system optimal exploitation through physics-based model predictive control, in: 2017 IEEE Manchester PowerTech, IEEE, 2017, pp. 1–6, http://dx.doi.org/10.1109/PTC.2017.7981145.

[16] H. Perez, N. Shahmohammadhamedani, S. Moura, Enhanced performance of li-ion batteries via modified reference governors and electrochemical models, IEEE/ASME Trans. Mechatronics 20 (4) (2015) 1511–1520, http://dx.doi.org/10.1109/TMECH.2014.2379695.

[17] L. Wikander, B. Fridholm, S. Gros, T. Wik, Ideal benefits of exceeding fixed voltage limits on lithium-ion batteries with increasing cycle age, J. Power Sources 441 (2019) 227179, http://dx.doi.org/10.1016/j.jpowsour.2019.227179.

[18] M. Doyle, T.F. Fuller, J. Newman, Modeling of galvanostatic charge and discharge of the lithium/polymer/insertion cell, J. Electrochem. Soc. 140 (6) (1993) 1526.

[19] T.F. Fuller, M. Doyle, J. Newman, Simulation and optimization of the dual lithium ion insertion cell, J. Electrochem. Soc. 141 (1) (1994) 1.

[20] G. Ning, B.N. Popov, Cycle life modeling of lithium-ion batteries, J. Electrochem. Soc. 151 (10) (2004) A1584, http://dx.doi.org/10.1149/1.1787631.

[21] S. Santhanagopalan, Q. Guo, P. Ramadass, R.E. White, Review of models for predicting the cycling performance of lithium ion batteries, J. Power Sources 156 (2) (2006) 620–628, http://dx.doi.org/10.1016/j.jpowsour.2005.05.070.

[22] C.-H. Chen, F. Brosa Planella, K. O'Regan, D. Gastol, W.D. Widanage, E. Kendrick, Development of experimental techniques for parameterization of multi-scale lithium-ion battery models, J. Electrochem. Soc. 167 (8) (2020) 080534, http://dx.doi.org/10.1149/1945-7111/ab9050.

[23] M. Ecker, T.K.D. Tran, P. Dechent, S. Kabitz, A. Warnecke, D.U. Sauer, Parameterization of a physico-chemical model of a lithium-ion battery: I. Determination of parameters, J. Electrochem. Soc. 162 (9) (2015) A1836–A1848, http://dx.doi.org/10.1149/2.0551509jes.

[24] M. Ecker, S. Kabitz, I. Laresgoiti, D.U. Sauer, Parameterization of a physico-chemical model of a Lithium-ion battery: II. Model validation, J. Electrochem. Soc. 162 (9) (2015) A1849–A1857, http://dx.doi.org/10.1149/2.0541509jes.

[25] J. Schmalstieg, C. Rahe, M. Ecker, D.U. Sauer, Full cell parameterization of a high-power Lithium-ion battery for a physico-chemical model: Part I. Physical and electrochemical parameters, J. Electrochem. Soc. 165 (16) (2018) A3799–A3810, http://dx.doi.org/10.1149/2.0321816jes.

[26] J. Schmalstieg, D.U. Sauer, Full cell parameterization of a high-power Lithium-ion battery for a physico-chemical model: Part II. Thermal parameters and validation, J. Electrochem. Soc. 165 (16) (2018) A3811–A3819, http://dx.doi.org/10.1149/2.0331816jes.

[27] T. Kim, W. Song, D.-Y. Son, L.K. Ono, Y. Qi, Lithium-ion batteries: outlook on present, future, and hybridized technologies, J. Mater. Chem. A 7 (7) (2019) 2942–2964, http://dx.doi.org/10.1039/C8TA10513H.

[28] D.L. Wood, J. Li, S.J. An, Formation challenges of Lithium-ion battery manufacturing, Joule 3 (12) (2019) 2884–2888, http://dx.doi.org/10.1016/j.joule.2019.11.002.

[29] S. Krüger, C. Hanisch, A. Kwade, M. Winter, S. Nowak, Effect of impurities caused by a recycling process on the electrochemical performance of $Li[Ni_{0.33}Co_{0.33}Mn_{0.33}]O_2$, J. Electroanal. Soc. 726 (2014) 91–96, http://dx.doi.org/10.1016/j.jelechem.2014.05.017.

[30] K. Uddin, S. Perera, W. Widanage, L. Somerville, J. Marco, Characterising Lithium-ion battery degradation through the identification and tracking of electrochemical battery model parameters, Batteries 2 (2) (2016) 13, http://dx.doi.org/10.3390/batteries2020013.

[31] L. Ljung, System Identification: Theory for the User, second ed., in: Wiley Encyclopedia of Electrical and Electronics Engineering, Prentice-Hall, New Jersey, 1999.

[32] J. Schoukens, L. Ljung, Nonlinear system identification: A user-oriented road map, IEEE Control Syst. Mag. 39 (6) (2019) 28–99, http://dx.doi.org/10.1109/MCS.2019.2938121.

[33] L. Ljung, Approaches to identification of nonlinear systems, in: Proceedings of the 29th Chinese Control Conference, IEEE, 2010, pp. 1–5.

[34] R. De Coninck, F. Magnusson, J. Åkesson, L. Helsen, Toolbox for development and validation of grey-box building models for forecasting and control, J. Build. Perform. Simul. 9 (3) (2016) 288–303, http://dx.doi.org/10.1080/19401493.2015.1046933.

[35] M. Torchio, L. Magni, R.B. Gopaluni, R.D. Braatz, D.M. Raimondo, LIONSIMBA: A Matlab framework based on a finite volume model suitable for Li-ion battery design, simulation, and control, J. Electrochem. Soc. 163 (7) (2016) A1192–A1205, http://dx.doi.org/10.1149/2.0291607jes.

[36] F. Ljungberg, Estimation of Nonlinear Greybox Models for Marine Applications, vol. 1880, Linköping University Electronic Press, 2020, http://dx.doi.org/10.3384/lic.diva-165828.

[37] D.C. López C, G. Wozny, A. Flores-Tlacuahuac, R. Vasquez-Medrano, V.M. Zavala, A computational framework for identifiability and ill-conditioning analysis of Lithium-ion battery models, Ind. Eng. Chem. Res. 55 (11) (2016) 3026–3042, http://dx.doi.org/10.1021/acs.iecr.5b03910.

[38] M. Box, Bias in nonlinear estimation, J. R. Stat. Soc. Ser. B Stat. Methodol. 33 (2) (1971) 171–190.

[39] A.M. Bizeray, J.-H. Kim, S.R. Duncan, D.A. Howey, Identifiability and parameter estimation of the single particle Lithium-ion battery model, IEEE Trans. Control Syst. Technol. 27 (5) (2019) 1862–1877, http://dx.doi.org/10.1109/TCST.2018.2838097.

[40] M. Ye, M. Hill, Global sensitivity analysis for uncertain parameters, models, and scenarios, in: G.P. Petropoulos, P.K. Srivastava (Eds.), Sensitivity Analysis in Earth Observation Modelling, Elsevier, 2017, pp. 177–210, http://dx.doi.org/10.1016/B978-0-12-803011-0.00010-0, (Chapter 10).

[41] R. Schenkendorf, X. Xie, M. Rehbein, S. Scholl, U. Krewer, The impact of global sensitivities and design measures in model-based optimal experimental design, Processes 6 (4) (2018) 27, http://dx.doi.org/10.3390/pr6040027.

[42] G. Franceschini, S. Macchietto, Model-based design of experiments for parameter precision: State of the art, Chem. Eng. Sci. 63 (19) (2008) 4846–4872, http://dx.doi.org/10.1016/j.ces.2007.11.034.

[43] D.P. Loucks, E. Van Beek, Water Resource Systems Planning and Management: An Introduction To Methods, Models, and Applications, Springer, 2017.

[44] J. Newman, W. Tiedemann, Porous-electrode theory with battery applications, AIChE J. 21 (1) (1975) 25–41, http://dx.doi.org/10.1002/aic.690210103.

[45] D.E. Stephenson, B.C. Walker, C.B. Skelton, E.P. Gorzkowski, D.J. Rowenhorst, D.R. Wheeler, Modeling 3D microstructure and ion transport in porous Li-ion battery electrodes, J. Electrochem. Soc. 158 (7) (2011) A781, http://dx.doi.org/10.1149/1.3579996.

[46] J. Newman, K.E. Thomas-Alyea, Electrochemical Systems, John Wiley & Sons, 2012.

[47] S.G. Marquis, V. Sulzer, R. Timms, C.P. Please, S.J. Chapman, An asymptotic derivation of a single particle model with electrolyte, J. Electrochem. Soc. 166 (15) (2019) A3693, http://dx.doi.org/10.1149/2.0341915jes.

[48] C.R. Pals, J. Newman, Thermal modeling of the Lithium/PolymerBattery: I . Discharge behavior of a single cell, J. Electrochem. Soc. 142 (10) (1995) 8, http://dx.doi.org/10.1149/1.2049974.

[49] K. Kumaresan, G. Sikha, R.E. White, Thermal model for a Li-ion cell, J. Electrochem. Soc. 155 (2) (2007) A164, http://dx.doi.org/10.1149/1.2817888.

[50] L. Zhang, C. Lyu, L. Wang, J. Zheng, W. Luo, K. Ma, Parallelized genetic identification of the thermal-electrochemical model for Lithium-ion battery, Adv. Mech. Eng. 5 (2013) 754653, http://dx.doi.org/10.1155/2013/754653.

[51] H. Chun, M. Kim, J. Kim, K. Kim, J. Yu, T. Kim, S. Han, Adaptive exploration harmony search for effective parameter estimation in an electrochemical Lithium-ion battery model, IEEE Access 7 (2019) 131501–131511, http://dx.doi.org/10.1109/ACCESS.2019.2940968.

[52] L. Zhang, L. Wang, G. Hinds, C. Lyu, J. Zheng, J. Li, Multi-objective optimization of lithium-ion battery model using genetic algorithm approach, J. Power Sources 270 (2014) 367–378, http://dx.doi.org/10.1016/j.jpowsour.2014.07.110.

[53] COMSOL AB, COMSOL Multiphysics®, www.comsol.com.

[54] V. Sulzer, S.G. Marquis, R. Timms, M. Robinson, S.J. Chapman, Python battery mathematical modelling (PyBaMM), J. Open Res. Softw. 9 (2021) p.14, http://dx.doi.org/10.5334/jors.309.

[55] R. Ahmed, M.E. Sayed, I. Arasaratnam, J. Tjong, S. Habibi, Reduced-order electrochemical model parameters identification and state of charge estimation for healthy and aged Li-ion batteries—Part II: Aged battery model and state of charge estimation, IEEE J. Emerg. Sel. Top. Power Electron. 2 (3) (2014) 678–690, http://dx.doi.org/10.1109/JESTPE.2014.2331062.

[56] B. Ng, P.T. Coman, W.E. Mustain, R.E. White, Non-destructive parameter extraction for a reduced order lumped electrochemical-thermal model for simulating Li-ion full-cells, J. Power Sources 445 (2020) 227296, http://dx.doi.org/10.1016/j.jpowsour.2019.227296.

[57] Y. Gao, X. Zhang, C. Zhu, B. Guo, Global parameter sensitivity analysis of electrochemical model for Lithium-ion batteries considering aging, IEEE/ASME Trans. Mechatronics 26 (3) (2021) 1283–1294, http://dx.doi.org/10.1109/TMECH.2021.3067923.

[58] R. Drummond, S.R. Duncan, Structural identifiability of a pseudo-2D Li-ion battery electrochemical model, IFAC-PapersOnLine 53 (2) (2020) 12452–12458, http://dx.doi.org/10.1016/j.ifacol.2020.12.1328.

[59] V. Ramadesigan, K. Chen, N.A. Burns, V. Boovaragavan, R.D. Braatz, V.R. Subramanian, Parameter estimation and capacity fade analysis of Lithium-ion batteries using reformulated models, J. Electrochem. Soc. 158 (9) (2011) A1048, http://dx.doi.org/10.1149/1.3609926.

[60] H. Lundgren, M. Behm, G. Lindbergh, Electrochemical characterization and temperature dependency of mass-transport properties of $LiPF_6$ in EC:DEC, J. Electrochem. Soc. 162 (3) (2014) A413–A420, http://dx.doi.org/10.1149/2.0641503jes.

[61] S. Schindler, M.A. Danzer, A novel mechanistic modeling framework for analysis of electrode balancing and degradation modes in commercial lithium-ion cells, J. Power Sources 343 (2017) 226–236, http://dx.doi.org/10.1016/j.jpowsour.2017.01.026.

[62] J. Christensen, J. Newman, Cyclable lithium and capacity loss in Li-ion cells, J. Electrochem. Soc. 152 (4) (2005) A818, http://dx.doi.org/10.1149/1.1870752.

[63] K. Mergo Mbeya, N. Damay, G. Friedrich, C. Forgez, M. Juston, Off-line method to determine the electrode balancing of Li-ion batteries, Math. Comput. Simulation 183 (2021) 34–47, http://dx.doi.org/10.1016/j.matcom.2020.02.013.

[64] C.R. Birkl, M.R. Roberts, E. McTurk, P.G. Bruce, D.A. Howey, Degradation diagnostics for lithium ion cells, J. Power Sources 341 (2017) 373–386, http://dx.doi.org/10.1016/j.jpowsour.2016.12.011.

[65] S. Müller, J. Eller, M. Ebner, C. Burns, J. Dahn, V. Wood, Quantifying inhomogeneity of lithium ion battery electrodes and its influence on electrochemical performance, J. Electrochem. Soc. 165 (2) (2018) A339–A344, http://dx.doi.org/10.1149/2.0311802jes.

[66] M. Klett, R. Eriksson, J. Groot, P. Svens, K. Ciosek Högström, R.W. Lindström, H. Berg, T. Gustafson, G. Lindbergh, K. Edström, Non-uniform aging of cycled commercial $LiFePO_4$//graphite cylindrical cells revealed by post-mortem analysis, J. Power Sources 257 (2014) 126–137, http://dx.doi.org/10.1016/j.jpowsour.2014.01.105.

[67] J. Sieg, M. Storch, J. Fath, A. Nuhic, J. Bandlow, B. Spier, D.U. Sauer, Local degradation and differential voltage analysis of aged lithium-ion pouch cells, J. Energy Storage 30 (2020) 101582, http://dx.doi.org/10.1016/j.est.2020.101582.

[68] N. Lin, X. Xie, R. Schenkendorf, U. Krewer, Efficient global sensitivity analysis of 3D multiphysics model for Li-ion batteries, J. Electrochem. Soc. 165 (7) (2018) A1169, http://dx.doi.org/10.1149/2.1301805jes.

[69] X. Lu, A. Bertei, D.P. Finegan, C. Tan, S.R. Daemi, J.S. Weaving, K.B. O'Regan, T.M. Heenan, G. Hinds, E. Kendrick, et al., 3D microstructure design of lithium-ion battery electrodes assisted by X-ray nano-computed tomography and modelling, Nature Commun. 11 (1) (2020) 1–13, http://dx.doi.org/10.1038/s41467-020-15811-x.

[70] M.M. Forouzan, B.A. Mazzeo, D.R. Wheeler, Modeling the effects of electrode microstructural heterogeneities on Li-ion battery performance and lifetime, J. Electrochem. Soc. 165 (10) (2018) A2127–A2144, http://dx.doi.org/10.1149/2.1281809jes.

[71] R.F. Muzic Jr., B.T. Christian, Evaluation of objective functions for estimation of kinetic parameters, Med. Phys. 33 (2) (2006) 342–353, http://dx.doi.org/10.1118/1.2135907.

[72] I.J. Myung, Tutorial on maximum likelihood estimation, J. Math. Psych. 47 (1) (2003) 90–100, http://dx.doi.org/10.1016/S0022-2496(02)00028-7.

[73] R. Masoudi, T. Uchida, J. McPhee, Parameter estimation of an electrochemistry-based lithium-ion battery model, J. Power Sources 291 (2015) 215–224, http://dx.doi.org/10.1016/j.jpowsour.2015.04.154.

[74] T. Weise, Global optimization algorithms-theory and application, in: E-Book, third ed., 2011, URL http://www.it-weise.de/projects/bookNew.pdf.

[75] P. Virtanen, R. Gommers, T.E. Oliphant, M. Haberland, T. Reddy, D. Cournapeau, E. Burovski, P. Peterson, W. Weckesser, J. Bright, et al., SciPy 1.0: Fundamental algorithms for scientific computing in Python, Nature Methods 17 (3) (2020) 261–272, http://dx.doi.org/10.1038/s41592-019-0686-2.

[76] J. Blank, K. Deb, Pymoo: Multi-objective optimization in python, IEEE Access 8 (2020) 89497–89509, http://dx.doi.org/10.1109/ACCESS.2020.2990567.

[77] I. Ahmadianfar, O. Bozorg-Haddad, X. Chu, Gradient-based optimizer: A new metaheuristic optimization algorithm, Inform. Sci. 540 (2020) 131–159, http://dx.doi.org/10.1016/j.ins.2020.06.037.

[78] Y. Bi, S.-Y. Choe, Automatic estimation of parameters of a reduced order electrochemical model for lithium-ion batteries at the beginning-of-life, in: 2018 IEEE Vehicle Power and Propulsion Conference (VPPC), IEEE, 2018, pp. 1–6, http://dx.doi.org/10.1109/VPPC.2018.8604954.

[79] L. Chen, R. Xu, W. Rao, H. Li, Y.P. Wang, T. Yang, H.B. Jiang, Electrochemical model parameter identification of lithium-ion battery with temperature and current dependence, Int. J. Electrochem. Sci. 14 (5) (2019) 4124–4143, http://dx.doi.org/10.20964/2019.05.05.

[80] Z. Deng, H. Deng, L. Yang, Y. Cai, X. Zhao, Implementation of reduced-order physics-based model and multi-parameters identification strategy for lithium-ion battery, Energy 138 (2017) 509–519, http://dx.doi.org/10.1016/j.energy.2017.07.069.

[81] G. Fan, Systematic parameter identification of a control-oriented electrochemical battery model and its application for state of charge estimation at various operating conditions, J. Power Sources 470 (2020) 228153, http://dx.doi.org/10.1016/j.jpowsour.2020.228153.

[82] J.C. Forman, S.J. Moura, J.L. Stein, H.K. Fathy, Genetic identification and fisher identifiability analysis of the Doyle–Fuller–Newman model from experimental cycling of a $LiFePO_4$ cell, J. Power Sources 210 (2012) 263–275, http://dx.doi.org/10.1016/j.jpowsour.2012.03.009.

[83] N. Jin, D.L. Danilov, P.M.J. Van den Hof, M.C.F. Donkers, Parameter estimation of an electrochemistry-based lithium-ion battery model using a two-step procedure and a parameter sensitivity analysis, Int. J. Energy Res. 42 (7) (2018) 2417–2430, http://dx.doi.org/10.1002/er.4022.

[84] A. Jokar, B. Rajabloo, M. Désilets, M. Lacroix, An inverse method for estimating the electrochemical parameters of Lithium-ion batteries: I. methodology, J. Electrochem. Soc. 163 (14) (2016) A2876–A2886, http://dx.doi.org/10.1149/2.0191614jes.

[85] J. Li, L. Zou, F. Tian, X. Dong, Z. Zou, H. Yang, Parameter identification of lithium-ion batteries model to predict discharge behaviors using heuristic algorithm, J. Electrochem. Soc. 163 (8) (2016) A1646, http://dx.doi.org/10.1149/2.0861608jes.

[86] Y. Ma, J. Ru, M. Yin, H. Chen, W. Zheng, Electrochemical modeling and parameter identification based on bacterial foraging optimization algorithm for lithium-ion batteries, J. Appl. Electrochem. 46 (11) (2016) 1119–1131, http://dx.doi.org/10.1007/s10800-016-0998-1.

[87] H. Pang, L. Mou, L. Guo, F. Zhang, Parameter identification and systematic validation of an enhanced single-particle model with aging degradation physics for Li-ion batteries, Electrochim. Acta 307 (2019) 474–487, http://dx.doi.org/10.1016/j.electacta.2019.03.199.

[88] Y. Qi, S. Kolluri, D.T. Schwartz, V.R. Subramanian, Estimating and identifying parameters from charge-discharge curves of Lithium-ion batteries, ECS Trans. 75 (20) (2017) 121–137, http://dx.doi.org/10.1149/07520.0121ecst.

[89] M.A. Rahman, S. Anwar, A. Izadian, Electrochemical model parameter identification of a lithium-ion battery using particle swarm optimization method, J. Power Sources 307 (2016) 86–97, http://dx.doi.org/10.1016/j.jpowsour.2015.12.083.

[90] B. Rajabloo, A. Jokar, M. Désilets, M. Lacroix, An inverse method for estimating the electrochemical parameters of Lithium-ion batteries: II: Implementation, J. Electrochem. Soc. 164 (2) (2017) A99–A105, http://dx.doi.org/10.1149/2.0221702jes.

[91] S.R. Reddy, M.K. Scharrer, F. Pichler, D. Watzenig, G.S. Dulikravich, Accelerating parameter estimation in Doyle–Fuller–Newman model for lithium-ion batteries, COMPEL - Int. J. Comput. Math. Electr. Electron. Eng. 38 (5) (2019) 1533–1544, http://dx.doi.org/10.1108/COMPEL-12-2018-0533.

[92] S. Santhanagopalan, Q. Guo, R.E. White, Parameter estimation and model discrimination for a lithium-ion cell, J. Electrochem. Soc. 154 (3) (2007) A198, http://dx.doi.org/10.1149/1.2422896.

[93] M.K. Scharrer, B. Suhr, D. Watzenig, A new space mapping parameter surrogate optimization for Lithium-Ion cell models, in: 4th Inverse Problems, Design and Optimization Symposium, 2013, pp. 26–28, http://dx.doi.org/10.13140/2.1.1116.9289.

[94] W.-J. Shen, H.-X. Li, Multi-scale parameter identification of lithium-ion battery electric models using a PSO-LM algorithm, Energies 10 (4) (2017) 432, http://dx.doi.org/10.3390/en10040432.

[95] J.H.A. Guillaume, J.D. Jakeman, S. Marsili-Libelli, M. Asher, P. Brunner, B. Croke, M.C. Hill, A.J. Jakeman, K.J. Keesman, S. Razavi, et al., Introductory overview of identifiability analysis: A guide to evaluating whether you have the right type of data for your modeling purpose, Environ. Model. Softw. 119 (2019) 418–432, http://dx.doi.org/10.1016/j.envsoft.2019.07.007.

[96] J. Nocedal, S. Wright, Numerical Optimization, second ed., Springer Science & Business Media, 2006, http://dx.doi.org/10.1007/978-0-387-40065-5.

[97] S. Boyd, L. Vandenberghe, Convex Optimization, Cambridge University Press, 2004.

[98] N. Xue, W. Du, A. Gupta, W. Shyy, A.M. Sastry, J.R.R.A. Martins, Optimization of a single Lithium-ion battery cell with a gradient-based algorithm, J. Electrochem. Soc. 160 (8) (2013) A1071–A1078, http://dx.doi.org/10.1149/2.036308jes.

[99] W. Mei, H. Chen, J. Sun, Q. Wang, The effect of electrode design parameters on battery performance and optimization of electrode thickness based on the electrochemical-thermal coupling model, Sustain. Energy Fuels 3 (1) (2019) 148–165, http://dx.doi.org/10.1039/c8se00503f.

[100] Y. Wang, L. Li, Li-ion battery dynamics model parameter estimation using datasheets and particle swarm optimization, Int. J. Energy Res. 40 (2016) 1050–1061, http://dx.doi.org/10.1002/er.3497.

[101] X.-S. Yang, S. Koziel, Computational optimization: An overview, Springer, 2011, pp. 1–11, http://dx.doi.org/10.1007/978-3-642-20859-1_1,

[102] T.R.B. Grandjean, L. Li, M.X. Odio, W.D. Widanage, Global sensitivity analysis of the single particle lithium-ion battery model with electrolyte, in: 2019 IEEE Vehicle Power and Propulsion Conference (VPPC), IEEE, 2019, pp. 1–7, http://dx.doi.org/10.1109/VPPC46532.2019.8952455.

[103] Q. Lai, S. Jangra, H.J. Ahn, G. Kim, W.T. Joe, X. Lin, Analytical sensitivity analysis for battery electrochemical parameters, in: 2019 American Control Conference (ACC), IEEE, 2019, pp. 890–896, http://dx.doi.org/10.23919/ACC.2019.8814950.

[104] X. Zeng, L. Xu, Z. Deng, F. Feng, X. Hu, Global sensitivity analysis of battery single particle model parameters, in: 2019 IEEE Vehicle Power and Propulsion Conference (VPPC), IEEE, 2019, pp. 1–6, http://dx.doi.org/10.1109/VPPC46532.2019.8952424.

[105] J. Vazquez-Arenas, L.E. Gimenez, M. Fowler, T. Han, S.-k. Chen, A rapid estimation and sensitivity analysis of parameters describing the behavior of commercial Li-ion batteries including thermal analysis, Energy Convers. Manage. 87 (2014) 472–482, http://dx.doi.org/10.1016/j.enconman.2014.06.076.

[106] C. Edouard, M. Petit, C. Forgez, J. Bernard, R. Revel, Parameter sensitivity analysis of a simplified electrochemical and thermal model for Li-ion batteries aging, J. Power Sources 325 (2016) 482–494, http://dx.doi.org/10.1016/j.jpowsour.2016.06.030.

[107] W. Li, D. Cao, D. Jöst, F. Ringbeck, M. Kuipers, F. Frie, D.U. Sauer, Parameter sensitivity analysis of electrochemical model-based battery management systems for lithium-ion batteries, Appl. Energy 269 (2020) 115104, http://dx.doi.org/10.1016/j.apenergy.2020.115104.

[108] L. Zhang, C. Lyu, G. Hinds, L. Wang, W. Luo, J. Zheng, K. Ma, Parameter sensitivity analysis of cylindrical $LiFePO_4$ battery performance using multi-physics modeling, J. Electrochem. Soc. 161 (5) (2014) A762–A776, http://dx.doi.org/10.1149/2.048405jes.

[109] Y. Liu, S. Tang, L. Li, F. Liu, L. Jiang, M. Jia, Y. Ai, C. Yao, H. Gu, Simulation and parameter identification based on electrochemical-thermal coupling model of power lithium ion-battery, J. Alloys Compd. 844 (2020) 156003, http://dx.doi.org/10.1016/j.jallcom.2020.156003.

[110] M.F. Samadi, M. Saif, Identifiability analysis of an electrochemical model of Li-ion battery, in: 2016 American Control Conference (ACC), IEEE, 2016, pp. 3107–3112, http://dx.doi.org/10.1109/ACC.2016.7525395.

[111] F. Pianosi, F. Sarrazin, T. Wagener, A matlab toolbox for global sensitivity analysis, Environ. Model. Softw. 70 (2015) 80–85, http://dx.doi.org/10.1016/j.envsoft.2015.04.009.

[112] F. Cannavó, Sensitivity analysis for volcanic source modeling quality assessment and model selection, Comput. Geosci. 44 (2012) 52–59, http://dx.doi.org/10.1016/j.cageo.2012.03.008.

[113] K. Weise, L. Poßner, E. Müller, R. Gast, T.R. Knösche, Pygpc: A sensitivity and uncertainty analysis toolbox for Python, SoftwareX 11 (2020) 100450, http://dx.doi.org/10.1016/j.softx.2020.100450.

[114] J. Herman, W. Usher, SALib: AN open-source python library for sensitivity analysis, J. Open Source Softw. 2 (9) (2017) http://dx.doi.org/10.21105/joss.00097.

[115] H.M. Wainwright, S. Finsterle, Y. Jung, Q. Zhou, J.T. Birkholzer, Making sense of global sensitivity analyses, Comput. Geosci. 65 (2014) 84–94, http://dx.doi.org/10.1016/j.cageo.2013.06.006.

[116] F. Pianosi, K. Beven, J. Freer, J.W. Hall, J. Rougier, D.B. Stephenson, T. Wagener, Sensitivity analysis of environmental models: A systematic review with practical workflow, Environ. Model. Softw. 79 (2016) 214–232, http://dx.doi.org/10.1016/j.envsoft.2016.02.008.

[117] A. Saltelli, M. Ratto, T. Andres, F. Campolongo, J. Cariboni, D. Gatelli, M. Saisana, S. Tarantola, Global Sensitivity Analysis. The Primer, John Wiley & Sons, Chichester, UK, 2007, http://dx.doi.org/10.1002/9780470725184.

[118] S. Park, D. Kato, Z. Gima, R. Klein, S. Moura, Optimal experimental design for parameterization of an electrochemical Lithium-ion battery model, J. Electrochem. Soc. 165 (7) (2018) A1309–A1323, http://dx.doi.org/10.1149/2.0421807jes.

[119] A. Saltelli, K. Aleksankina, W. Becker, P. Fennell, F. Ferretti, N. Holst, S. Li, Q. Wu, Why so many published sensitivity analyses are false: A systematic review of sensitivity analysis practices, Environ. Model. Softw. 114 (2019) 29–39, http://dx.doi.org/10.1016/j.envsoft.2019.01.012.

[120] A. Saltelli, P. Annoni, How to avoid a perfunctory sensitivity analysis, Environ. Model. Softw. 25 (12) (2010) 1508–1517, http://dx.doi.org/10.1016/j.envsoft.2010.04.012.

[121] F. Campolongo, A. Saltelli, J. Cariboni, From screening to quantitative sensitivity analysis. A unified approach, Comput. Phys. Comm. 182 (4) (2011) 978–988, http://dx.doi.org/10.1016/j.cpc.2010.12.039.

[122] S. Kucherenko, M. Rodriguez-Fernandez, C. Pantelides, N. Shah, Monte Carlo evaluation of derivative-based global sensitivity measures, Reliab. Eng. Syst. Saf. 94 (7) (2009) 1135–1148, http://dx.doi.org/10.1016/j.ress.2008.05.006.

[123] A. Saltelli, Global sensitivity analysis: An introduction, in: Proceedings of the 4th International Conference on Sensitivity Analysis of Model Output (SAMO 2004), 2004, pp. 27–43.

[124] I.M. Sobol, Sensitivity analysis for non-linear mathematical models, Math. Model. Comput. Exp. 1 (1993) 407–414.

[125] T. Homma, A. Saltelli, Importance measures in global sensitivity analysis of nonlinear models, Reliab. Eng. Syst. Saf. 52 (1) (1996) 1–17, http://dx.doi.org/10.1016/0951-8320(96)00002-6.

[126] B. Sudret, Global sensitivity analysis using polynomial chaos expansions, Reliab. Eng. Syst. Saf. 93 (2008) 964–979, http://dx.doi.org/10.1016/j.ress.2007.04.002.

[127] A. Goshtasbi, J. Chen, J.R. Waldecker, S. Hirano, T. Ersal, Effective parameterization of PEM fuel cell models—Part I: Sensitivity analysis and parameter identifiability, J. Electrochem. Soc. 167 (4) (2020) 044504, http://dx.doi.org/10.1149/1945-7111/ab7091.

[128] J.C. Forman, S.J. Moura, J.L. Stein, H.K. Fathy, Genetic parameter identification of the Doyle-Fuller-Newman model from experimental cycling of a $LiFePO_4$ battery, in: Proceedings of the 2011 American Control Conference, IEEE, 2011, pp. 362–369, http://dx.doi.org/10.1109/ACC.2011.5991183.

[129] R. Bellman, K.J. Åström, On structural identifiability, Math. Biosci. 7 (3–4) (1970) 329–339, http://dx.doi.org/10.1016/0025-5564(70)90132-X.

[130] L. Ljung, T. Glad, On global identifiability for arbitrary model parametrizations, Automatica 30 (2) (1994) 265–276, http://dx.doi.org/10.1016/0005-1098(94)90029-9.

[131] Z. Khalik, M.C.F. Donkers, J. Sturm, H.J. Bergveld, Parameter estimation of the Doyle–Fuller–Newman model for Lithium-ion batteries by parameter normalization, grouping, and sensitivity analysis, J. Power Sources 499 (2021) 229901, http://dx.doi.org/10.1016/j.jpowsour.2021.229901.

[132] A. Goshtasbi, J. Chen, J.R. Waldecker, S. Hirano, T. Ersal, Effective parameterization of PEM fuel cell models—Part II: Robust parameter subset selection, robust optimal experimental design, and multi-step parameter identification algorithm, J. Electrochem. Soc. 167 (4) (2020) 044505, http://dx.doi.org/10.1149/1945-7111/ab7092.

[133] J. Liu, M. Rothenberger, S. Mendoza, P. Mishra, Y.-s. Jung, H.K. Fathy, Can an identifiability-optimizing test protocol improve the robustness of subsequent health-conscious lithium-ion battery control? an illustrative case study, in: 2016 American Control Conference (ACC), IEEE, 2016, pp. 6320–6325.

[134] A.P. Schmidt, M. Bitzer, A.W. Imre, L. Guzzella, Experiment-driven electrochemical modeling and systematic parameterization for a lithium-ion battery cell, J. Power Sources 195 (15) (2010) 5071–5080, http://dx.doi.org/10.1016/j.jpowsour.2010.02.029.

[135] D.C. López C., T. Barz, S. Körkel, G. Wozny, Nonlinear ill-posed problem analysis in model-based parameter estimation and experimental design, Comput. Chem. Eng. 77 (2015) 24–42, http://dx.doi.org/10.1016/j.compchemeng.2015.03.002.

[136] B.F. Lund, B.A. Foss, Parameter ranking by orthogonalization—Applied to nonlinear mechanistic models, Automatica 44 (1) (2008) 278–281, http://dx.doi.org/10.1016/j.automatica.2007.04.006.

[137] J. Forman, J. Stein, H. Fathy, Optimization of dynamic battery paramter characterization experiments via differential evolution, in: 2013 American Control Conference, IEEE, 2013, pp. 867–874, http://dx.doi.org/10.1109/ACC.2013.6579945.

[138] A. Pozzi, G. Ciaramella, S. Volkwein, D.M. Raimondo, Optimal design of experiments for a lithium-ion cell: Parameters identification of an isothermal single particle model with electrolyte dynamics, Ind. Eng. Chem. Res. 58 (3) (2019) 1286–1299, http://dx.doi.org/10.1021/acs.iecr.8b04580.

[139] A. Pozzi, X. Xie, D.M. Raimondo, R. Schenkendorf, Global sensitivity methods for design of experiments in lithium-ion battery context, IFAC-PapersOnLine 53 (2) (2020) 7248–7255, http://dx.doi.org/10.1016/j.ifacol.2020.12.558.

[140] F. Emmert-Streib, Z. Yang, H. Feng, S. Tripathi, M. Dehmer, An introductory review of deep learning for prediction models with big data, Frontiers Artificial Intelligence 3 (2020) 4, http://dx.doi.org/10.3389/frai.2020.00004.

[141] G. James, D. Witten, T. Hastie, R. Tibshirani, Support Vector Machines, Springer, 2021, pp. 367–402, http://dx.doi.org/10.1007/978-1-0716-1418-1_9.

[142] M. Kim, H. Chun, J. Kim, K. Kim, J. Yu, T. Kim, S. Han, Data-efficient parameter identification of electrochemical lithium-ion battery model using deep Bayesian harmony search, Appl. Energy 254 (2019) 113644, http://dx.doi.org/10.1016/j.apenergy.2019.113644.

[143] H. Chun, J. Kim, J. Yu, S. Han, Real-time parameter estimation of an electrochemical Lithium-ion battery model using a long short-term memory network, IEEE Access 8 (2020) 81789–81799, http://dx.doi.org/10.1109/ACCESS.2020.2991124.

[144] A. Jokar, B. Rajabloo, M. Désilets, M. Lacroix, An on-line electrochemical parameter estimation study of Lithium-ion batteries using neural networks, ECS Trans. 75 (20) (2017) 73–87, http://dx.doi.org/10.1149/07520.0073ecst.

[145] M. Abadi, A. Agarwal, P. Barham, E. Brevdo, Z. Chen, C. Citro, G.S. Corrado, A. Davis, J. Dean, M. Devin, et al., Tensorflow: Large-scale machine learning on heterogeneous distributed systems, 2016, arXiv preprint arXiv:1603.04467.

[146] A. Paszke, S. Gross, F. Massa, A. Lerer, J. Bradbury, G. Chanan, T. Killeen, Z. Lin, N. Gimelshein, L. Antiga, et al., Pytorch: An imperative style, high-performance deep learning library, Adv. Neural Inf. Process. Syst. 32 (2019) 8026–8037.

[147] F. Pedregosa, G. Varoquaux, A. Gramfort, V. Michel, B. Thirion, O. Grisel, M. Blondel, P. Prettenhofer, R. Weiss, V. Dubourg, et al., Scikit-learn: Machine learning in python, J. Mach. Learn. Res. 12 (2011) 2825–2830.

[148] O. Simeone, A very brief introduction to machine learning with applications to communication systems, IEEE Trans. Cogn. Commun. Netw. 4 (4) (2018) 648–664, http://dx.doi.org/10.1109/TCCN.2018.2881442.

[149] M. Aykol, C.B. Gopal, A. Anapolsky, P.K. Herring, B. van Vlijmen, M.D. Berliner, M.Z. Bazant, R.D. Braatz, W.C. Chueh, B.D. Storey, Perspective—combining physics and machine learning to predict battery lifetime, J. Electrochem. Soc. 168 (3) (2021) 030525, http://dx.doi.org/10.1149/1945-7111/abec55.

[150] A.J. Bard, L.R. Faulkner, Electrochemical Methods: Fundamentals and Applications, second ed., John Wiley & Sons, New York, 2001.

[151] T. Waldmann, A. Iturrondobeitia, M. Kasper, N. Ghanbari, F. Aguesse, E. Bekaert, L. Daniel, S. Genies, I. Jiménez Gordon, M.W. Löble, E. De Vito, M. Wohlfahrt-Mehrens, Review—Post-mortem analysis of aged Lithium-ion batteries: Disassembly methodology and physico-chemical analysis techniques, J. Electrochem. Soc. 163 (10) (2016) A2149–A2164, http://dx.doi.org/10.1149/2.1211609jes.

[152] C. Merlet, A.C. Forse, J.M. Griffin, D. Frenkel, C.P. Grey, Lattice simulation method to model diffusion and NMR spectra in porous materials, J. Chem. Phys. 142 (9) (2015) http://dx.doi.org/10.1063/1.4913368.

[153] M. Månsson, J. Sugiyama, Muon-spin relaxation study on Li- and Na-diffusion in solids, Phys. Scr. 88 (6) (2013) http://dx.doi.org/10.1088/0031-8949/88/06/068509.

[154] M. Ebner, V. Wood, Tool for tortuosity estimation in Lithium ion battery porous electrodes, J. Electrochem. Soc. 162 (2) (2014) A3064–A3070, http://dx.doi.org/10.1149/2.0111502jes.

[155] C.J. Wen, B.A. Boukamp, R.A. Huggins, W. Weppner, Thermodynamic and mass transport properties of LiAl, J. Electrochem. Soc. 126 (12) (1979) 2258, http://dx.doi.org/10.1149/1.2128939.

[156] M.E. Orazem, B. Tribollet, Electrochemical Impedance Spectroscopy, second ed., John Wiley & Sons, Hoboken, New Jersey, 2017.